Doctoral Dissertation (Shinshu University)

Studies on functionalization of silk material by graphene oxide through self-assembly technology

March 2018

Jiangchao Song

Table of contents

List of Figure

Chapter 1：Introduction

Chapter 1 Introduction

Bombyx mori silk(The following is abbreviated as silk), a protein fiber derived from *Bombyx mori* silkworm cocoons, is known to be one of the strongest natural biomaterials[1]. Silk, has been employed for many years in textile in China. Silk protein is a natural macromolecular material composed of 18 kinds of amino acids, among which the content of glycine (43~ 46%), alanine (25~30%) and serine (12%) is about 80% of the total amino acid [2-4]. It is soft and shiny, and is known as the "fiber queen". Silk protein is often used as textile raw materials because of its good heat preservation, hygroscopicity, and moisture. Because of its soft, elegant, comfortable wearing and superior thermal performance, its textiles are popular among the public. Silk fabric is very popular in many overseas markets due to its excellent mechanical properties, luster, smoothness and comfort properties.

In addition, silk protein has stable physical and chemical properties, unique biodegradability and biocompatibility, which make it a very promising biological material [5-7]. At present, the preparation and development of new silk protein composites have developed rapidly and have been applied in many fields such as medicine, materials, food and environmental protection [8-10]. In order to meet some specific requirements across different fields, silk with enhanced mechanical properties is always required. A lot of new strategies include gene transfection, variations in spinning process and chemical or physical modifications of the silk. In recent years, scientists have developed a variety of methods for modification or enhancements of fibroin protein, such as regenerated silk method[11-13], the feeding and breeding improved environment law[14], mechanical drawing method[15-18], chemical grafting method and feeding the rearing method[19-25].

These methods have certain influence on nature of silk fiber, such as weakening mechanical properties of regenerated silk fiber, or affecting fiber's spinnability, or making fibers losing the unique properties of silk such as luster, softness, and so on.

These limitations restricts the application and development of silk fibroin composites. It is precious to prepare the fast durable functional silk fibroin bio-composite material, silk composite fiber or regenerated silk composite fiber with specific function, while retained the excellent characteristics of the natural silk as textile fiber material.

1.1 Structure and properties of silk fiber

Different from cotton and wool containing various substances, silk fibers are mainly composed of long-chain polypeptides. Silk protein is secreted by the silkworm. The length of silk protein secreted by each silkworm is 1000 ~1500 meters. Silk protein is the smallest, the softest and the lightest natural protein fiber in nature. Silk protein fiber has incomparable advantages over other synthetic fiber such as the low cost in production. The silk fiber is composed of silk protein and sericin protein: each silk protein fiber contains 70 to 75 percent of the silk protein, including 20 ~ 25% of silk glue and 5% of impurities (carbohydrate and pigment etc.)[26, 27]. Silk fiber (SF) is a naturally created protein fiber, mainly consisting of a gummy outer layer (sericin) and two core filaments (fibroin)[28]. As shown in **Figure 1.1**, the silk protein has distinct structure: triangular cross-section.

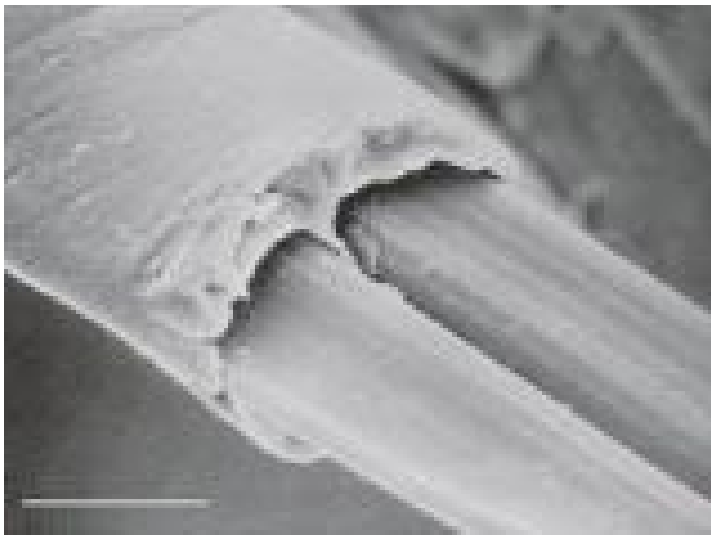

Figure 1.1 Unwashed native Bombyx mori silkworm silk[15]

Sericin is an amorphous protein that can be removed by the degumming process. Silk fibroin is composed of numerous minute fibrils, which could be separated into β-sheet crystals with strong hydrogen bonding and a non-crystalline (amorphous) region with varying degrees of hydrogen bonding[29]. The synergistic effect of sericin and fibroin protein plays an important role in the protection of silkworm larvae[30]. Silk fibroin is a main component to provide mechanical properties of silk protein. Silk protein is the most valuable research component; sericin protein is a water-soluble globular protein, is a kind of potential biological allergens, often with the reeling process in hot water was removed[31].

Silk fibroin is the main body of silk protein, with good biodegradability and biocompatibility[32]. Silk fibroin is a fibrous protein, including 900 ~ 1400 fibrils with a diameter of 1 μm, and along the longitudinal axis alignment (fibril is composed of the micro fibril, microfibril with a diameter of 10 ~ 15 nm), formed silk fibroin fibers with a diameter of 10 ~ 18 μm. The molecular weight of silk protein is very high, besides, molecular structure and molecular interaction are extremely complex. The silk protein is composed of the heavy chain (H chain, a molecular weight of 391 kDa), light chain (L chain, molecular weight 28 kDa) and P25 protein (molecular weight of 25 kDa).The heavy chain contains a large amount of glycine, and the light chain contains more alanine, glutamate, and phenylalanine. The heavy chain contains 11 crystalline and non-crystalline regions, with the light chain combined with the disulfide covalent bond and the molar ratio is 6:1. The P25 protein is connected by hydrophobic interaction with them[33]. The confirmation of silk fibroin molecules is composed of Silk I structure and Silk II structure. Silk I structure contains random coil and α-helix, and Silk II structure is mainly antiparallel β-sheet [34-36]. In the three conformations, the antiparallel β-sheet energy is the lowest and therefore the most stable.

The amino acid sequence in the crystalline region of the silk fibroin is mainly composed of glycine residues alternating with alanine and serine; the sequence in the amorphous region contains a tyrosine-rich domain[37, 38]. Silk fibroin fibers gain

smoothness and clear surfaces with good chemical activity, which can be easily combined with other functional materials [39-43]. And SFs are known to be one of the strongest natural fibers with excellent mechanical properties and have been used for textiles in the last several millennia [44, 45]. In general, the ultimate fracture strength of natural silk fiber is between 300 and 740 Mpa, and the fracture elongation is around 20%.

1.2 Silk fibroin Nanocomposite material

In natural biological silk, the mechanical properties of silk fibroin fiber are second only to natural spider silk. Compared to spider silk, silkworm silk protein is cheaper and more productive. Although silk has excellent mechanical properties and good biocompatibility, from the application point of view, natural silk fiber is currently used only in the field of textile and surgical suture area, the performance of a single to a certain extent, which limits the application of natural silk fiber. Therefore, in recent years, many researchers employed through a variety of technical treatment or adopt the method of integration with other functional materials, to modify functions of silk material. New function lead to new applications of silk fiber and improve the added value of natural silk. In this case, the new features of silk different from the conventional application are being discovered, based on the unique small size effect, surface effect and biological effect of nanomaterial. Therefore, the study of nanomaterials of silk is becoming a hot research area.

1.2.1 Spinning method of regenerated silk fibroin solution

Spinning method of regeneration silk fibroin solution is the process of converting the silk fibroin from the fiber to the solution and then into the fiber. During this process the silk fiber is dissolved into a protein solution, and then the silk protein solution is transformed into a silk fiber process by spinning. The content of β-sheet in fiber has great influence on mechanical properties of silk fibers. The silk fibers obtained by

solution regeneration method are smooth and uniform, but the mechanical properties are not as good as the raw silk fiber.

Generally speaking, the regenerated silk fibroin fiber is prepared through stretch spinning of silk fibroin solution[46], wet spinning [13, 47-52], dry spinning [53-58], and electrospinning[59-63], and so on. In order to improve the mechanical properties of the fibroin fiber, the researchers usually add nanomaterials to the silk fibroin solution before the spinning process as an enhancer. Common nano enhancers include carbon nanotubes, graphene, metal nanomaterials, etc. There are a lot of researchers on the regenerated silk fibroin fiber, and the kinds of literature have been summarized in detail [57, 64-66]. Therefore, this paper just introduces a few representative studies and the latest development.

Pan et al. added a small amount of titanium dioxide nanoparticles to the silk protein solution, and the silk protein/titanium dioxide composite fiber was obtained by dry spinning. The results show that the fiber is more resilient than silk fiber[12]. Pan et al. made the carbon nanotubes mixed with silk fibroin solution, through the electrostatic spinning technology to obtain the silk fibroin/carbon nanotube composite fiber, and the Raman images showed that carbon nanotubes were dispersed homogeneously in silk fibroin fibers [11].

Fibers of regenerated silk fibroin (RSF) are usually brittle and weak. Y Bai et al. prepared composite fibers of RSF reinforced via functional graphene oxide (FGO) with high strength by the wet spinning. The greatest force at the hybrid fibers was 697 ± 22 MPa up to break, which is a 58.7% improvement over the breakage force of pure RSF silk fiber[13]. Yifeng Huang et al. and Salvador A. C. et al. provided a new methodology to produce regenerated silk fibroin films as a good candidate material for usages in controlled release[43].

The smooth and uniform silk protein fiber can be obtained by means of dissolution and regeneration method; at the same time, after simple treatment, the enhancement agent can be distributed evenly to the inside of the fibroin fiber, thus obtain the

composite fiber material with uniform performance. After years of development and continuous improvement, the preparation of silk fibroin fiber has become more and more mature.

There is no doubt that when adding inorganic compounds in the proper regenerated silk fibroin spinning solution such as carbon nanotubes[11, 67-69], graphene[70-74], nanotitanium oxide[12, 75-77], nanohydroxyapatite[76, 78-82], montmorillonite[83, 84], even gold[70, 85] or silver[86, 87] nanoparticles, as long as the regenerated silk fibroin fiber can be smoothly spun nanofibers in spinning process under the appropriate condition, the performance has been improved more or less. However, the value is far from the expectation. Compared with natural silk, the regenerated fiber by this method has a large gap in mechanical properties, and it has no spinnability, which limits the scope and scale of its application. In addition, it leads to the longer cycle, higher requirements for instruments and solvents, and higher costs. Furthermore, a high concentration of salts as solvents will have a corrosive effect on the instrument, shortening the service life of the instrument.

1.2.2 New silk fiber via feeding silkworm functional nanomaterials

The method of feeding and rearing silkworm is a new method for the development of in-situ enhanced silk. Nanomaterials have unique properties, such as surface effect, small size effect, and quantum confinement effect, etc., which lead to its unique optical, electric, magnetic, thermal and mechanical properties. With the development of science and technology, nanomaterials are becoming more and more popular. In recent years, the researches on the usage of nanomaterials feeding method more to improve the performance of silk fibroin mechanics research has achieved rapid development, involving the nanomaterials mainly include fluorescent dye molecules，ferrosoferric oxide, carbon nanotubes, graphene, and titanium dioxide, and so on.

At first, Tansil et al. fed silkworm rhodamine functional fluorescent dye molecules, such as to gain with fluorescent colour cocoon. The results showed that dye molecules

exist in Bombyx mori silk fibroin, which is obviously different from ordinary color cocoons (the normal colored cocoon pigment molecules exist in silk glue)[19, 20]. In 2014, Anuya et al. further studied this experiment, they found that the proper molecular weight and hydrophilicity of the dye were the key to the color cocoons. It also found that a large number of dye molecules were present in the silk fibroin when the silkworm was fed Direct acid fast red and Mordant black 17, which showed that after the feeding of exogenous substances can participate in silkworm silk protein synthesis in the body and the assembly process, and the rearing method enhancing silk by subsequent added food laid a theoretical basis for the study of dynamic performance[21].

In 2014, Wang et al. were able to obtain the magnetic silk fibroin fiber by spraying the silkworm with the nano-grade ferrosoferric oxide (Fe_3O_4). Fe_3O_4 resulted in the reconstruction of some proteins on the surface of the silk fibroin. The silk fibroin fiber not only has good magnetic properties, but also has great mechanical properties and thermal stability, and in addition, the thermogravimetric analysis indicates that a small amount of trioxide is present in the fibroin fiber [22].

In addition, Wang et al. have coated the surface of mulberry leaf with MWCNT and fed the silkworm. The maximum fracture strength of silk protein fiber was 1.69 Gpa, 24 % higher than the blank group silk fiber, and the fracture elongation rate was 24 %. The mechanical properties of silk protein fiber were comparable to spider silk. The MWCNT are embedded within the silk fibroin, and the cross-section of the silk protein fiber is changed from a triangle to an ellipse. The contents of Silk I structure, thermal stability and conductivity of the Silk protein fiber are significantly improved due to the existence of MWCNT[23]. Qi Wang et al. reported mechanically enhanced silk directly collected from Bombyx mori larval silkworms fed with single-walled carbon nanotubes (SWNTs) and graphene. However, they also found that parts of the fed carbon nanomaterials were incorporated into the as-spun silk fibers, whereas the others went into the excrement of silkworms[25].

The above research shows that: (1) nanomaterials can be entered into silk by the metabolism of silkworm;(2) the embedding of functional nanomaterials is the fundamental cause of enhancing silk fibroin synthesis in situ.(3) silkworm feeding method can be used to synthesize silk protein/functional nanomaterials in situ, which is of constructive significance for the preparation of new biomaterials. Silkworm feeding method forms the silk fibroin/functional nanomaterials and composite materials through setting new functional materials to silk fibroin. The existence of nanomaterials can not only enhance the mechanical properties of the silk fibroin, but also makes the silk fibroin molecules with the performance of the nanomaterials. The method brings a new way to study the new performance of silk, and poses a great challenge in the development of technology about finding the right dose and examine individual differences of feeding quantity, and it is also a considerable challenge to keep the health of silkworms during the feeding period. Under the existing conditions, it will have a long way to go from small-scale rearing laboratory experiment to industrialized large-scale preparation of high-performance silk.

Regenerated silk fibroin fiber can be turned into the functional fiber via blending nanocomposites by the means of dissolution and regeneration method. However, under the existing process conditions, the regenerated fiber has a large gap in mechanical properties, even if the carbon nanotubes or graphene are added. The most important thing is that the regenerated silk lost a lot of excellent properties of natural silk because its internal microstructure has been destroyed in the regenerated silk fiber process, which directly results in the fact that the regenerated fibers are usually not spinnable. From the angle of textile science, defects in the fiber are quite obvious.

As for silkworm feeding method, it can be used to synthesize silk protein/functional nanomaterials in situ, which is of constructive significance for the preparation of new biomaterials. To some extent, we are optimistic. Nevertheless, under the existing conditions, even if we don’t consider about the production scale and quantity requirements, it is a great challenge to produce uniform functional silk. Now

we can only look forward to the further development of technology and the joint efforts of researchers in this area.

1.3 Graphene and graphene-based materials

Graphene and graphene-based materials have recently gained extensive interests for their good application potential in composite nanomaterials because of their unique physicochemical properties. Graphene is a single atom thick sheet made out of carbon atoms arranged in a honeycomb structure, which is the thinnest, strongest and stiffest material and has excellent heat and electronic conductivity, remarkably outperforming metals and metal composites[88-92]. Because of the poor affinity to natural fibers, naked functional nanoparticle coatings on natural fibers usually suffer from a function decrease under external physical and chemical stimuli, thereby leading to a poor function durability.

Similar to graphene, graphene oxides (GOs) also received extensive attention due to their similar structural properties. Generally, the main difference between graphene and GOs is the addition of oxygen atoms bound with the carbon scaffold[93]. Although GOs lost their electronic conductivity after oxidation, they inherit mechanical good properties from graphene. Besides, GOs possesses comparative advantages including good solubility in water and ease to tailor surface properties by functionalization, because of their particular surface functional groups such as hydroxyl and carboxyl groups[94-99]. Therefore, GOs gain certain advantages in medicine, adsorbing materials, sensors, functional composites etc. One typical case is the preparation of macroscopic multifunctional graphene-based hydrogels and aerogels in aqueous solution through reduction of GOs by ferrous ions and in situ attachment of nanoparticles on GOs. Such functional hydrogels possess excellent adsorption capacity for oil and metal ions[100].

With the excellent performance of graphene and graphene-based nanomaterials more and more found in recent years, graphene research has been widely involved in various fields of scientific research. The latest research reports on graphene materials

each year are growing up particularly and have been summarized in detail in the literature [101-142].

1.4 Silk fibroin and graphene / graphene-based materials

Silk, a protein-based natural polymer, is a flexible but strong material. Graphene oxide has so many hydroxyl and carboxyl groups, which is easy to react with the amino groups of the silk. It is a good strategy to prepare graphene and silk composite fibers served as the carrier of functional composite fibers.

Silk fibroin and graphene are both promising biomaterials described in the bibliography [39, 90, 143-148]. Hybrid scaffolds combining their properties could be attractive for tissue engineering applications [41, 146, 149, 150]. Salvador A. C. et al. provided a new methodology to produce electrospun fibroin scaffolds coated with graphene materials for application in biomedicine. The excellent biocompatibility of silk fibroin meshes was maintained after coating with graphene, being the proliferation results equal in all the treatments 7 days after the seeding (Tukey, $p > 0.05$) [146]. Graphene oxide has been uniformly adsorbed on silk-fibroin meshes and then chemically reduced to get a conductive, electroactive and very stable coating. Used as a self-supported working electrode in NaCl aqueous solution, the coated mesh supports the electrochemical characterization of the adsorbed graphene[151]. Silk protein nanofibers adhered on reduced graphene oxide (rGO) sheets are used as templates to regulate the formation of nanostructured iron oxide composites to develop a simple but effective strategy for the formation of metal oxide nanomaterials with superior performance, achieving porous nanorod structures that could not be attained in control experiments[152].

In the specific R & D process, silk fiber as a biomedical material, plays a key role in the design and synthesis of nanocomposite materials with controllable process, loading with nanoparticles dispersed on the surface of the chains. Silk fiber is often used as the first choice of bio-material for researchers from various fields [144, 145,

153-159]. Kook In Han et al. prepared flexible silk fiber (SF) coated with graphene oxide (GO) via electrostatic force without adhesive intermediates, which showed the feasibility of capacitive humidity sensor [160]. Liu, Ying et al. developed a flexible, simple-preparation, and low-cost graphene-silk pressure sensor based on soft silk substrate through thermal reduction, which can achieve the sensitivity value of 0.4 kPa^{-1}, and the measurement range can be as high as 140 kPa[161].

1.5 The purpose of this study

In order to obtain functional silk fiber, one of the effective means is coating the silk fibers with specific functional materials, such as organic materials and nanomaterials. When specific functional materials are attached on the outer surface, the obtained biological fibers can exhibit the combined properties of the original components. However, the structure of silk is single, which limits the application of silk materials.

In this case, we aim to design and develop a coaxial cable model and multilayer composite silk nanofibers, the synergistic effect of nanomaterials can be the better, given the silk fiber more new features and new applications, and as far as possible to retain the characteristics of silk fiber. Preserving the original characteristics and shape of silk provides infinite possibilities for the development and utilization of the textile field, and even more fields in the future, for example, wearable sensors for pulse, blood pressure, temperature and humidity, and so on.

So we go back to the source of the problem and our original intention, how can we hit such a goal? 1. Understanding the compatibility between natural silk and the functional nanomaterials (including graphene-based materials and functional nanoparticles) is essential to advance the use of silk in functional applications. 2. How to assemble nanocomposite fiber to achieve the quantitative controllability is also an unavoidable problem.

We have to turn to graphene oxide instead of graphene, because a large number of functional groups of graphene oxides sheets can react with the functional groups of silk

to produce crosslinking reactions, besides, they can absorb each other through the opposite charges under the certain solution conditions. Luckily, hyperbranched poly(amide-amino) (HBPAA) can enhance the reaction between GOs and silk fiber, which here serves as a strong guiding agent and glue because of their comparative advantages including cationic and amphipathic characteristics, three-dimensional structure, and dense amino end groups that can capture and fix negatively charged hydroxyl/carboxyl-contained GOs nanosheets compared to linear cationic electrolytes. It is worth noting that the final GO-coated silk composite fiber can be reduced to graphene-silk composite fiber according to the specific needs.

When we come to the quantitative controllability of the coating, layer by layer (LbL) self-assembly technology is considered as an advisable choice. Due to direct specific interactions and/or indirect interactions in their environment, it is feasible to achieve the process of self-assembly by the spontaneous organization of discrete components such molecules and NPs. The organization independent building blocks into ordered macroscopic structures need direct interactions or indirect interactions. Self-assembly of nanoparticles has been identified as an important process where the building blocks spontaneously organize into ordered structures by thermodynamic and other constraints[162]. This technique has been used for a long time and has been reported in a lot of literature [163-170], so no more details here. As for our case, silk is tough, but it becomes soft when exposed to water. Here a strong affinity of amine-functionalized Graphene oxide (AFGO) was designed, by coating the silk fibers with AFGO by LbL self-assembly technique onto the silk fibers to prepare of AFGO @ silk composite.

To sum up, graphene oxide coated silk material can be made of silk composite fiber through the layer by layer self-assembly technology, which not only makes the compatibility between natural silk and the functional nanomaterials, but also achieves the quantitative controllability. Meanwhile, the characteristics of silk fiber will be retained as far as possible.

1.6 Composition of this study

In this study, self-assembly strategies were developed to coat functional nanoparticles onto the surface of silk fibers in the controllable and environmental-friendly way. And then, a special LbL assembly technology was developed to prepare a tightly-adhered GOs coating. In particular, a GOs coating was prepared by cycle impregnation of two separate solutions of HBPAA and GOs. The developed LbL self-assembly technology may provide a controllable approach to coat GOs on the surface of biological fibers and graphene-based functional materials. At the same time, the prepared graphene and silk composite fiber can serve as the carrier of functional composite fibers, which has increased the chances of more choices to develop multi-functional composite fibers.

In Chapter 2, graphene oxide (GO)-coated silk fibers were fabricated through HBPAA-induced LbL self-assembly technology.

The closely adhered GOs coatings were achieved by circular incubation with solutions of HBPAA and GOs, with HBPAA serving as the "molecular glue" that could bind single or multi-layered GOs to the surface of silk fibers. The surface's chemical and physical properties of designed GOs /HBPAA-coated silk fibers were also characterized. In the experiments, GOs nanosheets were synthesized by a modified Hummers' method and were characterized by atomic force microscopy (AFM), transmission electron microscopy (TEM), X-ray diffraction (XRD), and X-ray photoelectron spectroscopy (XPS). Owing to the positive charges and abundant amino end groups of HBPAA, our developed technology was able to tightly bind GOs to the silk surface and control their loading capacity. The Fourier transform infrared (FT-IR) spectroscopy, XPS, XRD, thermos-gravimetric characterizations confirmed the attachment of HBPAA and GOs. With the increased density of GOs coatings, a silk surface in a small part was observed by Field emission scanning electron microscopy

(FESEM), to check the situation of GOs spreading on the surface of silk fibers and any self-folding though excessive stacking.

In chapter 3, GO-encapsulated Ag NP-coated silk fibers with hierarchical coaxial cable structure were fabricated by the molecule-directed self-assembly.

For protecting AgNP coatings from detachment, we designed the graphene oxide (GO)-encapsulated Ag nanoparticle (AgNP)-coated silk fibers with GO serving as the protective films through HBPAA-directed self-assembly. By introducing two dimensional GO nanosheets, a robust, hard, and closely-fitted protective films can be achieved on the fiber surfaces through self-stacked of GOs. To design a well-defined hierarchical structure, silk fibers were hierarchically coated with HBPAA-capped AgNPs (HBPAA/AgNPs) and GOs by successively impregnating the fibers in the solutions of HBPAA/AgNPs and GOs. In such structure, HBPAA served as "a double-sided tape" not only gluing AgNPs to the fiber surfaces but also adhere GOs to the surfaces of HBPAA/AgNPs. The developed coaxial cable-structured coatings could isolate Ag nanocoatings from external stimuli, opening a potential route to improve the function persistence and biosafety of AgNP-coated bio-textiles. As-prepared GOs by a modified Hummer' method and AgNPs were studied by TEM and AFM. The fact of HBPAA/AgNPs coatings encapsulated by GOs was examined FESEM. GOs coated to metallic AgNP surfaces was characterized by XPS and XRD.

In chapter 4, Fabrication of hierarchical structured graphene oxide-Fe_3O_4 hybrid nanosheets and Ag nanoparticles bimetallic coated silk fibers were fabricated through self-assembly.

To design and fabrication of well-organized hierarchical structured graphene oxide (GO)-Fe_3O_4 hybrid nanosheets and Ag nanoparticles (AgNPs), bimetallic coated silk fibers via a facile and simple assembly technology remain a significant challenge. Here we prepared novel hierarchical structured GO-Fe_3O_4NPs/AgNPs bimetallic coated silk

fibers via a special electrostatic self-assembly technology using positively charged AgNPs and negatively charged GO-Fe_3O_4NPs as the building blocks. Specifically, GO-Fe_3O_4NPs/AgNPs bimetallic coated silk fibers were facilely obtained by sequential impregnation with solutions of HBPAA-capped AgNPs and citric acid-capped GO-Fe_3O_4NPs. In the present work, special hierarchical structured GO-Fe_3O_4NPs/AgNPs bimetallic coated silk fibers have been prepared via a simple electrostatic self-assembly technology. Silk fibers were sequentially immersed in solutions of positively charged AgNPs and negatively charged GO-Fe_3O_4NPs as the building blocks. The excellent magnetic property and durable antibacterial property of the as-prepared bimetallic coated silk fibers will be studied further. Morphological studies of the as-prepared GO-Fe_3O_4NPs hybrid nanosheets was conducted by TEM and high-resolution TEM. The surface of pristine SF, GOs, AgNPs@SFs, GO-Fe_3O_4NPs nanosheets and GO-Fe_3O_4NPs/AgNPs@SFs were observed by FESEM. As-prepared hierarchical structured silk fibers were characterized by XRD, SEM, and FESEM.

Chapter 5 summarizes the conclusion of this study.

References

[1] Tao H, Kaplan DL, Omenetto FG. Silk Materials – A Road to Sustainable High Technology. Advanced materials. 2012;24:2824-37.

[2] Davarpanah S, Mahmoodi NM, Arami M, Bahrami H, Mazaheri F. Environmentally friendly surface modification of silk fiber: Chitosan grafting and dyeing. Applied Surface Science. 2009;255:4171-6.

[3] Zhong J, Ma M, Li W, Zhou J, Yan Z, He D. Self-assembly of regenerated silk fibroin from random coil nanostructures to antiparallel β-sheet nanostructures. Biopolymers. 2014;101:1181-92.

[4] Hashimoto T, Taniguchi Y, Kameda T, Tamada Y, Kurosu H. Changes in the properties and protein structure of silk fibroin molecules in autoclaved fabrics. Polymer Degradation & Stability. 2015;112:20-6.

[5] Kundu B, Rajkhowa R, Kundu SC, Wang X. Silk fibroin biomaterials for tissue regenerations. Advanced Drug Delivery Reviews. 2013;65:457.

[6] Zhao H, Heusler E, Jones G, Li L, Werner V, Germershaus O, et al. Decoration of silk fibroin by click chemistry for biomedical application. Journal of Structural Biology. 2014;186:420-30.

[7] Chen Q, Liu X, Zhao P, Sun Y, Zhao X, Xiong Y, et al. GC/MS-based metabolomic studies reveal key roles of glycine in regulating silk synthesis in silkworm, Bombyx mori. Insect Biochemistry & Molecular Biology. 2015;57:41.

[8] Xiao S, Wang Z, Ma H, Yang H, Xu W. Effective removal of dyes from aqueous solution using ultrafine silk fibroin powder. Advanced Powder Technology. 2014;25:574-81.

[9] Zhang Z, Qu Y, Li X, Zhang S, Wei Q, Shi Y, et al. Electrophoretic deposition of tetracycline modified silk fibroin coatings for functionalization of titanium surfaces. Applied Surface Science. 2014;303:255-62.

[10] Wang HY, Chen YY, Zhang YQ. Processing and characterization of powdered silk

micro- and nanofibers by ultrasonication. Materials Science & Engineering C Materials for Biological Applications. 2015;48:444.

[11] Pan H, Zhang Y, Hang Y, Shao H, Hu X, Xu Y, et al. Significantly reinforced composite fibers electrospun from silk fibroin/carbon nanotube aqueous solutions. Biomacromolecules. 2012;13:2859-67.

[12] Pan H, Zhang Y, Shao H, Hu X, Li X, Tian F, et al. Nanoconfined crystallites toughen artificial silk. Journal of Materials Chemistry B. 2014;2:1408-14.

[13] Hu X, Li J, Bai Y. Fabrication of high strength graphene/regenerated silk fibroin composite fibers by wet spinning. Materials Letters. 2017;194:224-6.

[14] Zhao HP, Feng XQ, Shi HJ. Variability in mechanical properties of Bombyx mori silk. Materials Science & Engineering C. 2007;27:675-83.

[15] Shao Z, Vollrath F. Surprising strength of silkworm silk. Nature. 2002;418:741.

[16] Khan MM, Morikawa H, Gotoh Y, Miura M, Ming Z, Sato Y, et al. Structural characteristics and properties of Bombyx mori silk fiber obtained by different artificial forcibly silking speeds. International Journal of Biological Macromolecules. 2008;42:264.

[17] Mortimer B, Holland C, Vollrath F. Forced Reeling of Bombyx mori Silk: Separating Behavior and Processing Conditions. Biomacromolecules. 2013;14:3653-9.

[18] Mortimer B, Guan J, Holland C, Porter D, Vollrath F. Linking naturally and unnaturally spun silks through the forced reeling of Bombyx mori. Acta Biomaterialia. 2015;11:247-55.

[19] Tansil NC, Li Y, Teng CP, Zhang S, Win KY, Chen X, et al. Intrinsically colored and luminescent silk. Advanced Materials. 2011;23:1463-6.

[20] Tansil NC, Koh LD, Han MY. Functional silk: colored and luminescent. Advanced Materials. 2012;24:1388-97.

[21] Nisal A, Trivedy K, Mohammad H, Panneri S, Gupta SS, Lele A, et al. Uptake of Azo Dyes into Silk Glands for Production of Colored Silk Cocoons Using a Green

Feeding Approach. Acs Sustainable Chemistry & Engineering. 2014;2:312-7.

[22] Wang JT, Li LL, Feng L, Li JF, Jiang LH, Shen Q. Directly obtaining pristine magnetic silk fibers from silkworm. International Journal of Biological Macromolecules. 2014;63:205.

[23] Wang JT, Li LL, Zhang MY, Liu SL, Jiang LH, Shen Q. Directly obtaining high strength silk fiber from silkworm by feeding carbon nanotubes. Materials Science & Engineering C Materials for Biological Applications. 2014;34:417.

[24] Cai L, Shao H, Hu X, Zhang Y. Reinforced and Ultraviolet Resistant Silks from Silkworms Fed with Titanium Dioxide Nanoparticles. Acs Sustainable Chemistry & Engineering. 2015;3:150907151650003.

[25] Wang Q, Wang C, Zhang M, Jian M, Zhang Y. Feeding Single-Walled Carbon Nanotubes or Graphene to Silkworms for Reinforced Silk Fibers. Nano Letters. 2016;16:6695.

[26] Wang F, Xu H, Wang Y, Wang R, Yuan L, Ding H, et al. Advanced silk material spun by a transgenic silkworm promotes cell proliferation for biomedical application. Acta Biomaterialia. 2014;10:4947.

[27] Koh LD, Cheng Y, Teng CP, Khin YW, Loh XJ, Tee SY, et al. Structures, mechanical properties and applications of silk fibroin materials. Progress in Polymer Science. 2015;46:86-110.

[28] Tansil NC, Koh LD, Han MY. Functional silk: colored and luminescent. Advanced Materials. 2012;24:1388-97.

[29] Wang Q, Wang C, Zhang M, Jian M, Zhang Y. Feeding Single-Walled Carbon Nanotubes or Graphene to Silkworms for Reinforced Silk Fibers. Nano letters. 2016;16:6695-700.

[30] Zhao HP, Feng XQ, Yu SW, Cui WZ, Zou FZ. Mechanical properties of silkworm cocoons. Polymer. 2005;46:9192-201.

[31] Jo YN, Um IC. Effects of solvent on the solution properties, structural characteristics and properties of silk sericin. International Journal of Biological

Macromolecules. 2015;78:287.

[32] Jia L, Guo L, Zhu J, Ma Y. Stability and cytocompatibility of silk fibroin-capped gold nanoparticles. Mater Sci Eng C Mater Biol Appl. 2014;43:231-6.

[33] Brown J, Lu CL, Coburn J, Kaplan DL. Impact of Silk Biomaterial Structure on Proteolysis. Acta Biomaterialia. 2015;11:212.

[34] Zhang F, Lu Q, Ming J, Dou H, Liu Z, Zuo B, et al. Silk dissolution and regeneration at the nanofibril scale. Journal of Materials Chemistry B. 2014;2:3879-85.

[35] Cheng G, Wang X, Tao S, Xia J, Xu S. Differences in regenerated silk fibroin prepared with different solvent systems: From structures to conformational changes. Journal of Applied Polymer Science. 2015;132.

[36] Zhang F, You X, Dou H, Liu Z, Zuo B, Zhang X. Facile Fabrication of Robust Silk Nanofibril Films via Direct Dissolution of Silk in CaCl2-Formic Acid Solution. Acs Applied Materials & Interfaces. 2015;7:3352.

[37] Drummy LF, Phillips DM, Stone MO, Farmer B, Naik RR. Thermally induced α-helix to β-sheet transition in regenerated silk fibers and films. Biomacromolecules. 2005;6:3328-33.

[38] Lin N, Meng Z, Toh GW, Zhen Y, Diao Y, Xu H, et al. Engineering of fluorescent emission of silk fibroin composite materials by material assembly. Small. 2015;11:1205-14.

[39] Kim D-H, Viventi J, Amsden JJ, Xiao J, Vigeland L, Kim Y-S, et al. Dissolvable films of silk fibroin for ultrathin conformal bio-integrated electronics. Nature materials. 2010;9:511-7.

[40] Correia C, Bhumiratana S, Yan L-P, Oliveira AL, Gimble JM, Rockwood D, et al. Development of silk-based scaffolds for tissue engineering of bone from human adipose-derived stem cells. Acta biomaterialia. 2012;8:2483-92.

[41] Mou Z-L, Duan L-M, Qi X-N, Zhang Z-Q. Preparation of silk fibroin/collagen/hydroxyapatite composite scaffold by particulate leaching method.

Materials Letters. 2013;105:189-91.

[42] Deng M, Huang Z, Zou Y, Yin G, Liu J, Gu J. Fabrication and neuron cytocompatibility of iron oxide nanoparticles coated with silk-fibroin peptides. Colloids Surf B Biointerfaces. 2014;116:465-71.

[43] Huang Y, Bailey K, Wang S, Feng X. Silk fibroin films for potential applications in controlled release. Reactive & Functional Polymers. 2017.

[44] Perea GB, Solanas C, Marí-Buyé N, Madurga R, Agulló-Rueda F, Muinelo A, et al. The apparent variability of silkworm (Bombyx mori) silk and its relationship with degumming. European Polymer Journal. 2016;78:129-40.

[45] Ling S, Jin K, Kaplan DL, Buehler MJ. Ultrathin Free-Standing Bombyx mori Silk Nanofibril Membranes. Nano letters. 2016;16:3795-800.

[46] Xie F, Zhang H, Shao H, Hu X. Effect of shearing on formation of silk fibers from regenerated Bombyx mori silk fibroin aqueous solution. International Journal of Biological Macromolecules. 2006;38:284.

[47] Matsumoto K, Uejima H, Iwasaki T, Sano Y, Sumino H. Studies on regenerated protein fibers. III. Production of regenerated silk fibroin fiber by the self‐dialyzing wet spinning method. Journal of Applied Polymer Science. 1996;60:503-11.

[48] Ha SW, Park YH, Hudson SM. Dissolution of Bombyx mori silk fibroin in the calcium nitrate tetrahydrate-methanol system and aspects of wet spinning of fibroin solution. Biomacromolecules. 2003;4:488-96.

[49] Ha SW, And AET, Hudson SM. Structural Studies of Bombyx mori Silk Fibroin during Regeneration from Solutions and Wet Fiber Spinning. Biomacromolecules. 2005;6:1722-31.

[50] Marsano E, Corsini P, Arosio C, Boschi A, Mormino M, Freddi G. Wet spinning of Bombyx mori silk fibroin dissolved in N-methyl morpholine N-oxide and properties of regenerated fibres. International Journal of Biological Macromolecules. 2005;37:179-88.

[51] Yan J, Zhou G, Knight DP, Shao Z, Chen X. Wet-Spinning of Regenerated Silk Fiber from Aqueous Silk Fibroin Solution: Discussion of Spinning Parameters. Biomacromolecules. 2010;11:1.

[52] Jacobsen MM, Li D, Rim NG, Backman D, Smith ML, Wong JY. Silk-fibronectin protein alloy fibres support cell adhesion and viability as a high strength, matrix fibre analogue. Scientific Reports. 2017;7:45653.

[53] Ma YL, Zhu JX, Shao HL, Hu XC. Methanol Induced Changes in Structure and Properties of Dry Spinning Fibers of Regenerated Silk Fibroin. Advanced Materials Research. 2011;335-336:908-11.

[54] Wei W, Zhang Y, Zhao Y, Luo J, Shao H, Hu X. Bio-inspired capillary dry spinning of regenerated silk fibroin aqueous solution. Materials Science & Engineering C. 2011;31:1602-8.

[55] Jin Y, Zhang Y, Hang Y, Shao H, Hu X. A simple process for dry spinning of regenerated silk fibroin aqueous solution. Journal of Materials Research. 2013;28:2897-902.

[56] Chao Z, Zhang Y, Shao H, Hu X. Hybrid Silk Fibers Dry-Spun from Regenerated Silk Fibroin/Graphene Oxide Aqueous Solutions. Acs Applied Materials & Interfaces. 2016;8:3349.

[57] Peng Q, Shao H, Hu X, Zhang Y. Microfluidic Dry-spinning and Characterization of Regenerated Silk Fibroin Fibers. J Vis Exp. 2017.

[58] Zhang C, Shao HL, Hu XC, Zhang YP. Effect of Draw Ratio on the Microstructure of Silk Fibroin/Graphene Oxide Hybrid Fibers. Materials Science Forum2017. p. 2214-23.

[59] Jin HJ, Chen J, Karageorgiou V, Altman GH, Kaplan DL. Human bone marrow stromal cell responses on electrospun silk fibroin mats. Biomaterials. 2004;25:1039-47.

[60] Min BM, Lee G, Kim SH, Nam YS, Lee TS, Park WH. Electrospinning of silk fibroin nanofibers and its effect on the adhesion and spreading of normal human

keratinocytes and fibroblasts in vitro. Biomaterials. 2004;25:1289.

[61] Catto V, Farè S, Cattaneo I, Figliuzzi M, Alessandrino A, Freddi G, et al. Small diameter electrospun silk fibroin vascular grafts: Mechanical properties, in vitro biodegradability, and in vivo biocompatibility. Materials Science & Engineering C. 2015;54:101.

[62] Ju HW, Lee OJ, Lee JM, Moon BM, Park HJ, Park YR, et al. Wound healing effect of electrospun silk fibroin nanomatrix in burn-model. International Journal of Biological Macromolecules. 2016;85:29.

[63] Singh BN, Panda NN, Pramanik K. A novel electrospinning approach to fabricate high strength aqueous silk fibroin nanofibers. International Journal of Biological Macromolecules. 2016;87:201-7.

[64] Leng B, Huang L, Shao Z. Chapter 5 - Inspiration from Natural Silks and Their Proteins: Elsevier Science & Technology; 2009.

[65] Fu C, Shao Z, Fritz V. ChemInform Abstract: Animal Silks: Their Structures, Properties and Artificial Production. Cheminform. 2010;41:6515.

[66] Kamalha E. Regenerated Silk Fibroin and Electrospun Fibers. 2016.

[67] Ko FK, Sukigara S, Gandhi M, Ayutsede J. Electrospun carbon nanotube reinforced silk fibers. US; 2007.

[68] Pan H, Zhang Y, Hang Y, Ding Y, Shao H, Hu X. Multiwalled carbon nanotube reinforced fibers electrospun from regenerated silk fibroin aqueous solutions. 2011.

[69] Lepore E, Bonaccorso F, Bruna M, Bosia F, Taioli S, Garberoglio G, et al. Silk reinforced with graphene or carbon nanotubes spun by spiders. Physics. 2015;4.

[70] Aktürk Ö, Kısmet K, Yastı AÇ, Kuru S, Duymuş ME, Kaya F, et al. Wet electrospun silk fibroin/gold nanoparticle 3D matrices for wound healing applications. Rsc Advances. 2016;6:13234-50.

[71] Aznar-Cervantes S, Martínez JG, Bernabeu-Esclapez A, Lozano-Pérez AA, Meseguer-Olmo L, Otero TF, et al. Fabrication of electrospun silk fibroin scaffolds coated with graphene oxide and reduced graphene for applications in biomedicine.

Bioelectrochemistry. 2016;108:36-45.

[72] Zhao Y, Gong J, Niu C, Wei Z, Shi J, Li G, et al. A new electrospun graphene-silk fibroin composite scaffolds for guiding Schwann cells. Journal of Biomaterials Science Polymer Edition. 2017:1-30.

[73] Yang Y, Ding X, Zou T, Peng G, Liu H, Fan Y. Preparation and characterization of electrospun graphene/silk fibroin conductive fibrous scaffolds. Rsc Advances. 2017;7:7954-63.

[74] Aznar-Cervantes S, Pagán A, Martínez JG, Bernabeu-Esclapez A, Otero TF, Meseguer-Olmo L, et al. Electrospun silk fibroin scaffolds coated with reduced graphene promote neurite outgrowth of PC-12 cells under electrical stimulation. Materials Science & Engineering C Materials for Biological Applications. 2017;79:315.

[75] Jao WC, Yang MC, Lin CH, Hsu CC. Fabrication and characterization of electrospun silk fibroin/TiO 2 nanofibrous mats for wound dressings. Polymers for Advanced Technologies. 2012;23:1066–76.

[76] Kim JH, Kim DK, Lee OJ, Ju HW, Lee JM, Moon BM, et al. Osteoinductive silk fibroin/titanium dioxide/hydroxyapatite hybrid scaffold for bone tissue engineering. International Journal of Biological Macromolecules. 2016;82:160.

[77] Johari N, Madaah Hosseini HR, Samadikuchaksaraei A. Optimized composition of nanocomposite scaffolds formed from silk fibroin and nano-TiO2 for bone tissue engineering. Materials Science & Engineering C. 2017;79:783-92.

[78] Kong XD, Cui FZ, Wang XM, Zhang M, Zhang W. Silk fibroin regulated mineralization of hydroxyapatite nanocrystals. Journal of Crystal Growth. 2004;270:197-202.

[79] Wei K, Li Y, Kim KO, Nakagawa Y, Kim BS, Abe K, et al. Fabrication of nano‐hydroxyapatite on electrospun silk fibroin nanofiber and their effects in osteoblastic behavior. Journal of Biomedical Materials Research Part A. 2011;97A:272-80.

[80] Ming J, Zuo B. A novel electrospun silk fibroin/hydroxyapatite hybrid nanofibers. Materials Chemistry & Physics. 2012;137:421-7.

[81] Paşcu EI, Stokes J, Mcguinness GB. Electrospun composites of PHBV, silk fibroin and nano-hydroxyapatite for bone tissue engineering. Materials Science & Engineering C Materials for Biological Applications. 2013;33:4905-16.

[82] Niu B, Li B, Gu Y, Shen X, Liu Y, Chen L. In vitro evaluation of electrospun silk fibroin/nano-hydroxyapatite/BMP-2 scaffolds for bone regeneration. Journal of Biomaterials Science Polymer Edition. 2017;28:257.

[83] Dang Q, Lu S, Yu S, Sun P, Yuan Z. Silk fibroin/montmorillonite nanocomposites: effect of pH on the conformational transition and clay dispersion. Biomacromolecules. 2010;11:1796-801.

[84] Kishimoto Y, Ito F, Usami H, Togawa E, Tsukada M, Morikawa H, et al. Nanocomposite of silk fibroin nanofiber and montmorillonite: Fabrication and morphology. International Journal of Biological Macromolecules. 2013;57:124-8.

[85] Cohenkarni T, Jeong KJ, Tsui JH, Reznor G, Mustata M, Wanunu M, et al. Nanocomposite Gold-Silk Nanofibers. Nano Letters. 2012;12:5403.

[86] Kang M, Jung R, Kim HS, Youk JH, Jin HJ. Silver nanoparticles incorporated electrospun silk fibers. J Nanosci Nanotechnol. 2007;7:3888-91.

[87] Uttayarat P, Jetawattana S, Suwanmala P, Eamsiri J, Tangthong T, Pongpat S. Antimicrobial electrospun silk fibroin mats with silver nanoparticles for wound dressing application. Fibers & Polymers. 2012;13:999-1006.

[88] Geim AK, Novoselov KS. The rise of graphene. Nat Mater. 2007;6:183-91.

[89] Paredes JI, Villar-Rodil S, Fernandez-Merino MJ, Guardia L, Martinez-Alonso A, Tascon JMD. Environmentally friendly approaches toward the mass production of processable graphene from graphite oxide. Journal of Materials Chemistry. 2011;21:298-306.

[90] Hu K, Gupta MK, Kulkarni DD, Tsukruk VV. Ultra-Robust Graphene Oxide-Silk Fibroin Nanocomposite Membranes. Advanced Materials. 2013;25:2301-7.

[91] Li J-L, Tang B, Yuan B, Sun L, Wang X-G. A review of optical imaging and therapy using nanosized graphene and graphene oxide. Biomaterials. 2013;34:9519-34.

[92] Georgakilas V, Tiwari JN, Kemp KC, Perman JA, Bourlinos AB, Kim KS, et al. Noncovalent Functionalization of Graphene and Graphene Oxide for Energy Materials, Biosensing, Catalytic, and Biomedical Applications. Chemical Reviews. 2016.

[93] Seah C-M, Vigolo B, Chai S-P, Mohamed AR. Mechanisms of graphene fabrication through plasma-induced layer-by-layer thinning. Carbon. 2016;105:496-509.

[94] Shan C, Yang H, Han D, Zhang Q, Ivaska A, Niu L. Water-soluble graphene covalently functionalized by biocompatible poly-L-lysine. Langmuir. 2009;25:12030-3.

[95] Ma J, Zhang J, Xiong Z, Yong Y, Zhao X. Preparation, characterization and antibacterial properties of silver-modified graphene oxide. Journal of Materials Chemistry. 2011;21:3350-2.

[96] Georgakilas V, Otyepka M, Bourlinos AB, Chandra V, Kim N, Kemp KC, et al. Functionalization of Graphene: Covalent and Non-Covalent Approaches, Derivatives and Applications. Chemical Reviews. 2012;112:6156-214.

[97] Qu Y, Ma M, Wang Z, Zhan G, Li B, Wang X, et al. Sensitive amperometric biosensor for phenolic compounds based on graphene–silk peptide/tyrosinase composite nanointerface. Biosensors and Bioelectronics. 2013;44:85-8.

[98] Maktedar SS, Mehetre SS, Singh M, Kale R. Ultrasound irradiation: A robust approach for direct functionalization of graphene oxide with thermal and antimicrobial aspects. Ultrasonics sonochemistry. 2014;21:1407-16.

[99] Suresh I, Chidambaram K, Vinod V, Rajender N, Venkateswara RM, Miroslav Č. Synthesis, characterization and optical properties of graphene oxide–polystyrene nanocomposites. Polymers for Advanced Technologies. 2015;26:214-22.

[100] Cong H-P, Ren X-C, Wang P, Yu S-H. Macroscopic Multifunctional

Graphene-Based Hydrogels and Aerogels by a Metal Ion Induced Self-Assembly Process. ACS Nano. 2012;6:2693-703.

[101] Cao YM, Qing-Kai WU, Department G. Application progress of graphene, graphene derivatives and graphene composites in tissue engineering. Journal of Shanghai Jiaotong University. 2017.

[102] Chen J, Hui XU. Research Progress of Graphene and Its Nanocomposites as Anodes for Lithium Ion Batteries. Materials Review. 2017.

[103] Gao Y, Wang J, Li J. Research Progress of Graphene Composites. 2017.

[104] Jang HS, Jeon JW, Kim BH. Recent Progress on Graphene-Based Materials for Hydrogen Storage. Polymerence & Technology. 2017;28.

[105] Jiang L, Wang JH, Han ZD. Domestic Research Progress in Graphene Oxide/Phenolic Formaldehyde Resin Composites. Journal of Harbin University of Science & Technology. 2017.

[106] Kumar R, Singh RK, Singh DP, Joanni E, Yadav RM, Moshkalev SA. Laser-assisted synthesis, reduction and micro-patterning of graphene: Recent progress and applications. Coordination Chemistry Reviews. 2017;342:34-79.

[107] Li JS, Hui H, Zhou YJ, Zhang CY, Li ZT. Research progress of graphene-based microwave absorbing materials in the last decade. Journal of Materials Research. 2017;32:1213-30.

[108] Li K, Zhang Y, Wang L, Zhang J. Research Progress of Electron Transfer Kinetics Based on Graphene Electrodes. Micronanoelectronic Technology. 2017.

[109] Liu S, Wang C, Cheng Q, Xia Z, Zhao W, Zhao H, et al. Progress of Protective Performance of Graphene Based Composite Coatings. Materials China. 2017;36:377-83.

[110] Ning-Li AN, Liu YX, Ren PG, Jia-Bin LI, Shu-Yun AN. Structural Construction and Application Progress of Graphene. Packaging Engineering. 2017.

[111] Pham VP, Jang HS, Whang D, Choi JY. Direct growth of graphene on rigid and flexible substrates: progress, applications, and challenges. Chemical Society

Reviews. 2017.

[112] Ren YL, Song H, Jiang ZY, Shao YQ, Liu SJ, Zhou S, et al. The Graphene and its Application Research Progress. Journal of Mudanjiang Normal University. 2017.

[113] Shen D, Jinhong YU, Jiang N, Zhan Z. Research Progress of Properties of Graphene/Epoxy Resin Composite. Hot Working Technology. 2017.

[114] Shengfei HU, Wei W, Liu Q, Zhang R. Research Progress on Preparation of Graphene by Supercritical Fluid Exfoliation. 2017.

[115] Tiwari A. Progress in the graphene research since 2010. Advanced Materials Letters. 2017;8:185-6.

[116] Wang T, Ge S, Periodontology DO, Stomatology HO, University S. Research progress on the application of graphene oxide in the field of biomedicine. International Journal of Stomatology. 2017.

[117] Wang Y, Wang X, Feng J. The Chemical Modification of Graphene and Recent Progress in Leather Industry. Leather Science & Engineering. 2017.

[118] Wang Y, Zhou JX, Cheng KM, Wu JH, Yang YS. Progress on Preparation, Microstructure and Property of Graphene Reinforced Aluminum Matrix Composite. Materials Science Forum2017.

[119] Wang Z, Ren PG, Ren F, Zhu GJ. Adsorption and Research Progress of Graphene and Composites. Packaging Engineering. 2017.

[120] Xie L, Xiong YZ, Luo Z, Zheng Q. Progress of Conductive Graphene/Polymer Composites. China Plastics Industry. 2017.

[121] Yang B, Zhou LH, Xiao-Yan MA. Research Progress on Application of Graphene in Solid Phase Extraction of Metal Ions. Guangzhou Chemical Industry. 2017.

[122] Yang H, Cui H, Tang W, Li Z, Han N, Xing F. A Critical Review on Research Progress of Graphene/Cement Based Composites. Composites Part A Applied Science & Manufacturing. 2017.

[123] Zhang P, Yuan T, Jiafeng R, Tan Z, Pang Y, Zheng S. Research progress on freestanding electrode based on graphene for supercapacitors. Electronic

Components & Materials. 2017.

[124] Zhang XS, Zhou QX, Technology HU, University LT. The progress in preparation of graphene by exfoliation of graphite. Carbon Techniques. 2017.

[125] Zhang Z, Xiang YU, Liu F. The Research Progress of Industrialization Synthesizes in Graphene Nano-sheet. Journal of New Industrialization. 2017.

[126] Zhao P, Fan S. Research Progress of Grapheneresonant Vibration Measurement. Metrology & Measurement Technology. 2017.

[127] Zhao S, Chen Y, Wang S, Rao Y, Shi X, Liu F, et al. Research Progress in Anti-Corrosion Coatings Containing Graphene. Journal of Changzhou University. 2017.

[128] Zheng Y, Cao N. Research Progress on Graphene Oxide Nanoribbons Nanohybrids and Graphene Nanoribbons. 2017.

[129] Bai RG, Ninan N, Muthoosamy K, Manickam S. Graphene: A Versatile Platform for Nanotheranostics and Tissue Engineering. Progress in Materials Science. 2017.

[130] Dong HM, Qian HH, Cheng LJ, Su ZT, Liu J, Wang WZ, et al. Research Progress in Graphene/Rubber Conducting Nanocomposites. Cailiao Gongcheng/journal of Materials Engineering. 2017;45:17-27.

[131] Fatemi SM, Baniasadi A, Moradi M. Recent progress in molecular simulation of nanoporous graphene membranes for gas separation. Journal- Korean Physical Society. 2017;71:54-62.

[132] Kim M, Hwang HM, Park GH, Lee H. Graphene-based composite electrodes for electrochemical energy storage devices: Recent progress and challenges. Flatchem. 2017.

[133] Li W, Ren RP. Research progress of graphene-based oil absorption materials. Xiandai Huagong/modern Chemical Industry. 2017;37:19-22 and 4.

[134] Morales-Narváez E, Sgobbi LF, Machado SAS, Merkoçi A. Graphene-encapsulated materials: Synthesis, applications and trends. Progress in Materials Science. 2017;86:1-24.

[135] Nika DL, Balandin AA. Phonons and thermal transport in graphene and graphene-based materials. Reports on Progress in Physics Physical Society. 2017;80:036502.

[136] Papageorgiou DG, Kinloch IA, Young RJ. Mechanical properties of graphene and graphene-based nanocomposites. Progress in Materials Science. 2017;90:75-127.

[137] Ping Y, Gong Y, Fu Q, Pan C. Preparation of three-dimensional graphene foam for high performance supercapacitors. Progress in Natural Science:Materials International. 2017;27.

[138] Punetha VD, Rana S, Yoo HJ, Chaurasia A, Jr ML, Ramasamy MS, et al. Functionalization of carbon nanomaterials for advanced polymer nanocomposites: A comparison study between CNT and graphene. Progress in Polymer Science. 2017;67:1-47.

[139] Tong L, Qiu F, Zeng T, Long J, Yang J, Wang R, et al. Recent progress in the preparation and application of quantum dots/graphene composite materials. Rsc Advances. 2017;7:47999-8018.

[140] Qi M, Li S, Du Y, Ye P, Han H, He Q, et al. Researchprogress of the graphene-based nano-composites. Gongneng Cailiao/journal of Functional Materials. 2017;48:03042-9.

[141] Wang Y, Zhou JX, Cheng KM, Wu JH, Yang YS. Progress on Preparation, Microstructure and Property of Graphene Reinforced Aluminum Matrix Composite. Materials Science Forum. 2017;898:917-32.

[142] Yu Q, Liang J, Yu Q, Liang J, Yu Q, Liang J. Progress in preparation and functionalization of graphene. 2017.

[143] Yukseloglu SM, Sokmen N, Canoglu S. Biomaterial applications of silk fibroin electrospun nanofibres. Microelectronic Engineering. 2015;146:43-7.

[144] Liu X, Yin G, Yi Z, Duan T. Silk Fiber as the Support and Reductant for the Facile Synthesis of Ag–Fe3O4 Nanocomposites and Its Antibacterial Properties. Materials. 2016;9:501.

[145] Xu S, Song J, Zhu C, Morikawa H. Graphene oxide-encapsulated Ag nanoparticle-coated silk fibers with hierarchical coaxial cable structure fabricated by the molecule-directed self-assembly. Materials Letters. 2016.

[146] Aznar-Cervantes S, Martinez JG, Bernabeu-Esclapez A, Lozano-Perez AA, Meseguer-Olmo L, Otero TF, et al. Fabrication of electrospun silk fibroin scaffolds coated with graphene oxide and reduced graphene for applications in biomedicine. Bioelectrochemistry. 2016;108:36-45.

[147] Melke J, Midha S, Ghosh S, Ito K, Hofmann S. Silk fibroin as biomaterial for bone tissue engineering. Acta Biomaterialia. 2016;31:1.

[148] Terada D, Yokoyama Y, Hattori S, Kobayashi H, Tamada Y. The outermost surface properties of silk fibroin films reflect ethanol-treatment conditions used in biomaterial preparation. Materials Science & Engineering C. 2016;58:119.

[149] Yang Y, Ding X, Zou T, Yao Y, Liu H, Fan Y. Fabrication and characterization of aligned graphene/silk fibroin nanofibrous scaffolds for nerve tissue regeneration. Journal of Controlled Release. 2017;259:e171.

[150] Liang Y, Li L, Wang L, Xu P, Gao Y, Fan Y, et al. Fabrication, characterization and biocompatibility evaluation of graphene/silk fibroin composite films. Gongneng Cailiao/journal of Functional Materials. 2017;48:07001-5.

[151] Martinez JG, Aznar-Cervantes S, Abel Lozano-Pérez A, Cenis JL, Otero TF. Graphene adsorbed on silk-fibroin meshes: Biomimetic and reversible conformational movements driven by reactions. Electrochimica Acta. 2016;209:521-8.

[152] Sheng W, Zhu G, Lu Q, Kaplan DL. Metal Oxide Nanomaterials with Nitrogen-Doped Graphene-Silk Nanofiber Complexes as Templates. Particle & Particle Systems Characterization. 2016;33:286-92.

[153] Fei X, Jia M, Du X, Yang Y, Zhang R, Shao Z, et al. Green synthesis of silk fibroin-silver nanoparticle composites with effective antibacterial and biofilm-disrupting properties. Biomacromolecules. 2013;14:4483-8.

[154] Xu S, Song J, Morikawa H, Chen Y, Lin H. Fabrication of hierarchical structured Fe3O4 and Ag nanoparticles dual-coated silk fibers through electrostatic self-assembly. Materials Letters. 2016;164:274-7.

[155] Chawla S, Kumar A, Admane P, Bandyopadhyay A, Ghosh S. Elucidating role of silk-gelatin bioink to recapitulate articular cartilage differentiation in 3D bioprinted constructs. Bioprinting. 2017.

[156] Seib FP. Silk nanoparticles—an emerging anticancer nanomedicine. 2017;4:239-58.

[157] Sharifiaghdam M, Faridimajidi R, Derakhshan MA, Chegeni A, Azami M. Preparation of collagen/polyurethane/knitted silk as a composite scaffold for tendon tissue engineering. Proceedings of the Institution of Mechanical Engineers Part H Journal of Engineering in Medicine. 2017:954411917697751.

[158] Yadav S, Gaba G. Mango Kernel Starch- A Natural Thickener for Screen Printing on Silk With Kachnar Bark Dye. 2017.

[159] Yang M. Silk-based biomaterials. Microsc Res Tech. 2017;80:321-30.

[160] Han KI, Kim S, Lee IG, Kim JP, Kim JH, Hong SW, et al. Compliment Graphene Oxide Coating on Silk Fiber Surface via Electrostatic Force for Capacitive Humidity Sensor Applications. Sensors. 2017;17:407.

[161] Liu Y, Tao LQ, Wang DY, Zhang TY, Yang Y, Ren TL. Flexible, highly sensitive pressure sensor with a wide range based on graphene-silk network structure. Applied Physics Letters. 2017;110:123508.

[162] Grzelczak M, Vermant J, Furst EM, Lizmarzán LM. Directed self-assembly of nanoparticles. Acs Nano. 2010;4:3591.

[163] Zhu YB, Gao CY, Liu YX, Gong YH, Shen JC. LBL Self-assembly of Chondroitin Sulfate and Collagen onto Poly(L-lactic acid) Surface for Improving Its Cytocompatibility with Endothelial Cells. Chemical Research in Chinese Universities. 2004;25:1347-50.

[164] Yang P, Li CL, Murase N. Highly photoluminescent multilayer QD-glass films

prepared by LbL self-assembly. Langmuir the Acs Journal of Surfaces & Colloids. 2005;21:8913.

[165] Zhang RJ, Cui JW, Lu DM, Hou WG. Study on high-efficiency fluorescent microcapsules doped with europium beta-diketone complex by LbL self-assembly. Chemical Communications. 2007;15:1547-9.

[166] Li X, Hu D, Huang K, Yang C. Hierarchical rough surfaces formed by LBL self-assembly for oil-water separation. Journal of Materials Chemistry A. 2014;2:11830-8.

[167] Starr BJ, Tarabara VV, Herrera-Robledo M, Zhou M, Roualdes S, Ayral A. Corrigendum to “Coating porous membranes with a photocatalyst: Comparison of LbL self-assembly and plasma-enhanced CVD techniques” [J. Membr. Sci. 514 (2016) 340–349]. Journal of Membrane Science. 2016;520:812-3.

[168] Sui C, Wang C, Wang Z, Xu Y, Gong E, Cheng T, et al. Different Coating on Electrospun Nanofiber via layer-by-layer self-assembly for Their Photocatalytic Activities. Colloids & Surfaces A Physicochemical & Engineering Aspects. 2017;529.

[169] Zhang D, Jiang C, Sun YE, Zhou Q. Layer-by-layer self-assembly of tricobalt tetroxide-polymer nanocomposite toward high-performance humidity-sensing. Journal of Alloys & Compounds. 2017;711:652-8.

[170] Zhao M, Yuan W, Li CM. Controlled self-assembly of Ni foam supported poly(ethyleneimine)/reduced graphene oxide three-dimensional composite electrodes with remarkable synergistic effects for efficient oxygen evolution. Journal of Materials Chemistry A. 2017;5.

Chapter 2： Preparation of graphene oxide-coated silk fibers through HBPAA [a molecular glue]-induced layer-by-layer self-assembly

Chapter 2 Preparation of graphene oxide-coated silk fibers through HBPAA [a molecular glue] -induced layer-by-layer self-assembly

2.1 Introduction

Silk fiber is a natural protein polymer that has been used as a textile fabric for thousands of years [1]. It received widespread attention for textile, surgical suture, drug delivery and tissue engineering due to its excellent mechanical properties, biodegradability and biocompatibility [2, 3]. In recent years, the functional finishing of Silk fiber has attracted great interest of many researchers. For instance, many metal nano particles (NPs) such as TiO_2 NPs [4], Ag NPs [5, 6] and Fe_3O_4 NPs [6, 7] have been successfully used to prepare metal NPs coated silk fibers. And these functionalized silk fibers were endowed with remarkable UV protection properties, antimicrobial properties and magnetic properties.

Graphene is a single atom thick sheet made out of carbon atoms arranged in a honeycomb structure, which is the thinnest, strongest and stiffest material and has excellent heat and electronic conductivity, remarkably outperforming metals and metal composites [8-12]. Graphene oxide (GO) is a kind of inorganic nano-materials. Although GOs lost their electronic conductivity after oxidation, they inherit good mechanical properties from graphene. Similar to graphene, graphene oxides (GOs) also received extensive attention due to their similar structural properties. Generally, the main difference between graphene and GOs is the addition of oxygen atoms bound with the carbon scaffold [13]. Besides, GOs possesses comparative advantages including good solubility in water and ease to tailor surface properties by functionalization based on their particular surface functional groups such as hydroxyl and carboxyl groups [14-19]. Therefore, GOs gain certain advantages in medicine, adsorbing materials, sensors, functional composites, etc. One typical case is the preparation of macroscopic

multifunctional graphene-based hydrogels and aerogels in aqueous solution through reduction of GOs by ferrous ions and in situ attachment of nanoparticles on GOs. Such functional hydrogels possess excellent adsorption capacity for oil and metal ions [20].

Graphene and GOs also have drawn the extensive attention of textile designers because of its outstanding physicochemical properties. Due to the excellent mechanical properties, the integration of graphene and their derivatives in natural biological fibers may improve their mechanical properties or electrical and thermal conductivity [21]. Interestingly, very recently, graphene and GOs were also reported to have good antibacterial activity. Liu, et al. found that GOs showed highest antibacterial activity compared with reduced GOs and graphite towards Escherichia coli and the mechanism [22] includes initial cell attachment on graphene-based nanomaterials, followed by cell membrane damage of bacteria caused by direct contact with the extremely sharp edge of GOs [23-25]. Notably, graphene is hydrophobic in nature and also cannot be dissolved in conventional organic solvents whereas the GO is hydrophilic. Nevertheless, the GO is easy to be reduced to graphene using various reducing agents [26-29]. This property is very useful for their application in functional textiles.

Generally speaking, the common strategy for functionalization of textile fibers with nanomaterials is dependent on water-based coating technology including pad-dry-baking finishing, spraying, in-situ deposition, sol-gel dipping. Thus, the initial coating of GOs nanosheets on textile fibers with subsequent reduction of GOs into graphene may overcome the poor dispersibility of graphene in water and enhance the electrical conductivity. However, GO is synthesized in strong acid and oxidant environment, which indicates in-situ deposition and sol-gel coating is not applicative. The existing problems for two former strategies are poor closeness, weak bonding strength between biomacromolecules and GOs, and inevitable enfoldment of nanosheets. An alternative solution is molecular-guided assembly technology, based on using functional molecules to guide and adhere nanosheets onto biological substrates.

In this paper, a special layer-by-layer (LbL) assembly technology[30] was

developed to prepare a tightly-adhered GOs coating. Particular, a GOs coating was prepared by cycle impregnation of two separate solutions of hyperbranched poly (amide-amino) (HBPAA) and GOs. Hyperbranched polyamides here serve as a strong guiding agent and glue because of their comparative advantages including cationic and amphipathic characteristics, three-dimensional structure, and dense amino end groups that can capture and fix negatively charged hydroxyl/carboxyl-contained GOs nanosheets compared to linear cationic electrolytes. We detailedly demonstrated LbL assembly process. The surface chemical and physical properties of designed GOs /HBPAA-coated silk fibers were also characterized.

2.2 Experimental methods

2.2.1. Materials

Silk fibers were obtained from the Ueda Fujimoto Co., Ltd (Japan). HBPAA was synthesized according to our previous research[31]. Graphite, which was supposed to expand to nearly 200 times its original size after being treated at about 1000^{o}C, Concentrated sulfuric acid (H_2SO_4, 98%), hydrogen peroxide (H_2O_2, 30%), and potassium permanganate ($KMnO_4$) were purchased from Wake Pure Chemical Industries CO., LTD. Dimethylformamide (DMF), Poly (diallyldimethylammonium chloride) (PDDA; Mw: 20000) and sodium polyacrylate (PAAS; Mw: 30000) were purchased from Aldrich. All other reagents were at least of analytical reagent grade and used without further purification. Distilled water was used in all the processes of aqueous solution preparations and washings.

2.2.2. Preparation of Graphene Oxides (GOs)

GOs were synthesized by oxidizing graphite powder using a modified Hummers method [32-34]. In the given process, graphite(2.0 g) and $NaNO_3$(1.0 g) were added to 50 mL of concentrated H_2SO_4(98%), and the mixture was mechanically stirred in an ice bath for 2 h. $KMnO_4$(7.3 g) was slowly added to the mixture, then 7 mL of H_2O_2 and

150 mL of deionized water were added respectively. Thus the color of the mixture changed from brown into the bright yellow. The mixture was filtered and washed several times with 3% HCl solution and deionized water. GO was vacuum-dried at 40°C for 24 h and obtained as brown solid. The obtained product was dispersed in 500 mL water through ultrasonication. In the end, solid form of GO was obtained by centrifugation and vacuum drying at 40°C for 24 h.

2.2.3. LbL assembly of HBPAA and GOs on silk fibers

GOs/HBPAA coated silk fibers were prepared by cycle impregnation of silk fibers with solutions of HBPAA and GOs. In brief, HBPAA-coated silk fibers were firstly prepared by adding silk fibers into 40 mL of 20 g/L of HBPAA aqueous solution and kept stirring at 70 ^{o}C for 30 min. The resulting HBPAA-coated silk fibers were then transferred to 100 mg/L of GOs solution and kept stirring for another 10 min at room temperature to completely uptake GOs. By repeating above processes, a dense GOs coating can be obtained. Notably, except for the first cycle, the coating of HBPAA on silk fibers were conducted at room temperature. Finally, the as-prepared GOs/HBPAA-coated silk fibers were dried and cured at 120 ^{o}C for 10 min.

2.2.4. Testing and analysis

2.2.4.1. Characterization of GOs

The morphology of graphene oxides was investigated using a JEOL-2100F transmission electron microscope (TEM) (JEOL, Japan) operating at an accelerating voltage of 120 kV. For Fourier transform infrared (FTIR) measurement, the graphene oxides solution was poured into acetone and the resulting precipitates were dried for characterization. The FTIR spectra were performed on a Shimadzu FTIR, IR Prestige-21 infrared spectrometer (Shimadzu, Japan). The surface chemical structure of the GOs was characterized by X-ray photoelectron spectroscopy (XPS) using an X-ray diffractometer (Krotos, Japan, AXIS Ultra DLD). The crystal structure of pristine and

modified Silk fibers was examined by an X-ray diffractometer (XRD) (Rigaku, Japan, R-AXIS D53C). And the instrument was calibrated with (CDFN-SRM675 Mica) prior to analysis.

2.2.4.2. Characterization of GOs/HBPAA-coated silk fibers

The morphology and size of the composite silk fibers were observed using a field-emission scanning electron microscope (FESEM) (Hitachi, Japan, S4800). The Fourier transform infrared (FT-IR) spectroscopic analysis was carried out using a Shimadzu FTIR (Shimadzu, Japan, IR Prestige-21). The surface chemical structure of the SF was characterized using an X-ray diffractometer (Krotos, Japan, AXIS Ultra DLD). The crystal structure of pristine and modified Silk fibers was examined by an X-ray diffractometer (XRD) (Rigaku, Japan, R-AXIS D53C). And the instrument was calibrated with (CDFN-SRM675 Mica) prior to analysis. Thermogravimetric analyses (TGA) were conducted on a TG 8120 (Rigaku Thermo Plus, Japan) at a heating rate of 10°C/min and a nitrogen flow rate of 150 mL/min.

2.3. Results and discussion

2.3.1. Properties of GOs

Prior to practice our concept, it should be noted that to apply a colloidal coating of two-dimensional nanomaterials on natural fibers, the nanomaterial should possess two important properties: high water stability and good flexibility to avoid possible precipitation and gain the adaptive capacity for complicated and rough silk surface by shape self-adaptation. Interestingly, GOs can fully meet above requirements due to their amphiphilic nature and nanoscale thickness.

In this study, GOs were synthesized by oxidizing graphite powder using a modified Hummers method. As displayed in **Figure 2.1 a**, the GOs showed excellent dispersibility in water and a lamellated liquid crystal phase with a brownish color that is derived from the nano-effect of GOs nanosheets. The synthetic GO solution can be

stored for several months, indicative of their good stability, attributing to the electrostatic repulsion among GOs. Furthermore, the GOs nanosheets consist of single layers whose size is ranged from hundreds of nanometers to several micrometers (see TEM photograph in **Figure 2.1 c**). As shown in **Figure 2.1 b**, the thickness of the GOs sheets was around 0.8 nm as measured by (AFM), suggesting the formation of a single-layered 2-D carbon nanosheet. The crystalline state was also analyzed by XPS and XRD. As shown in **Figure 2.1 d**, from XRD measurement, the characteristic peak at 11.3° (002), corresponding to a d-spacing of about 0.78 nm that is attributed to intercalation of water and other oxygen-containing groups trapped between GO sheets, agreeing well with that determined by AFM. The good chemical structure and nanoscale thickness of GOs ensure their further application in the surface coating of silk fibers.

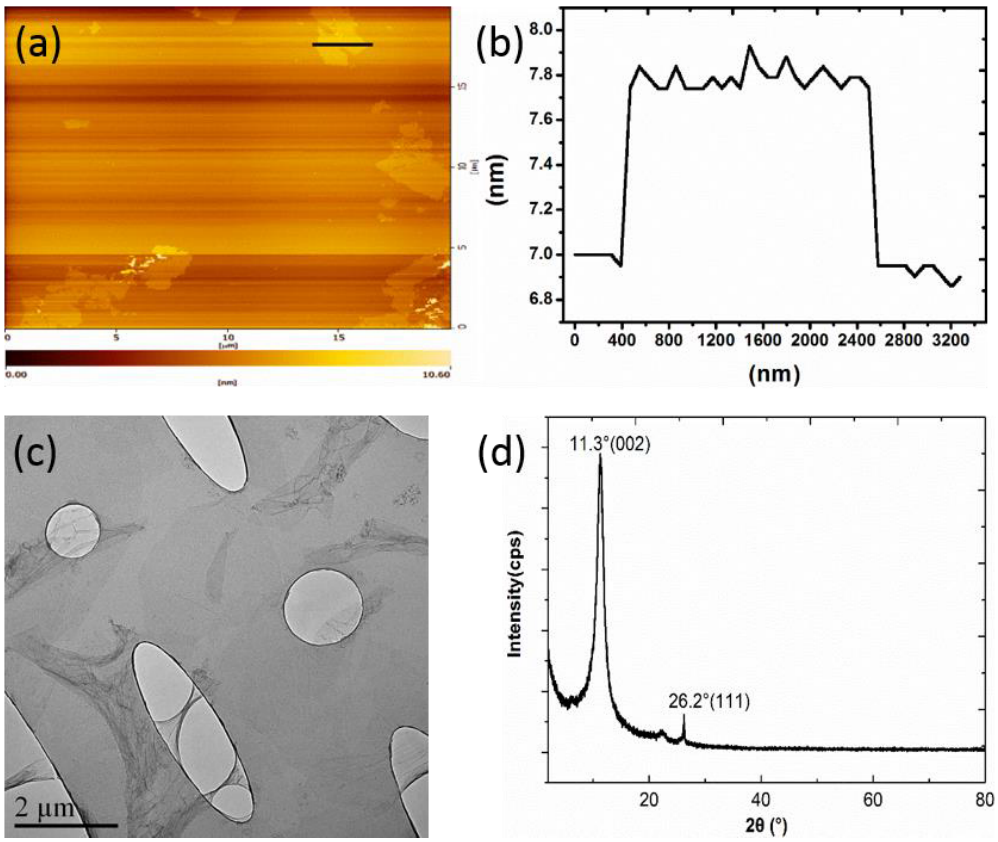

Figure 2. 1 (a) AFM analysis for topographical investigation of the GOs and (b) thicknesses of GOs films measured by AFM. (c) TEM photograph and (d) XRD spectrum of GOs.

2.3.2. LbL self-assembly of GOs on the surface of silk fibers

In comparison with zero-dimensional nanoparticles and one-dimensional nanowire, two dimensional GOs have distinct nature including microscale surface and atom-sized thickness. Therefore, the coating of GO nanosheets on similar micro-sized silk fibers need an effective means to control their spatial arrangement to avoid self-folding and to improve chemical affinity to silk fibers, due to their flexibility and strong mutual repulsion. Therefore, we here developed a bottom-up LbL self-assembly strategy with the purpose of steadily, efficiently, and uniformly spreading GOs on silk surface. The mechanism of the LBL self-assembly is shown in **Figure 2.2**. The main principle of this technology is the introduction of cationic amino-terminated HBPAAs onto silk surface to guide GOs to controllably assemble onto the silk surface by intermolecular force

between the HBPAA and the carboxyl-containing GOs sheet. Interestingly, GOs possesses excellent amphiphilicity. The plane of the GO sheet is hydrophobic because it mainly consists of hydrophobic C-C=C groups though it contains some hydrophilic OH and COOH side groups, while the edge is hydrophilic due to COOH and OH end groups. Therefore, the self-arrangement of the negatively charged GOs on positively charged HBPAAs on the surface of silk fibers is mainly dependent on their hydrophilic COOH and OH groups. Therefore, in the first circle of LbL self-assembly, GOs tend to monodispersed on the surface of silk fibers because of their strong mutual electrostatic repulsion. This property can promote the uniformity of GOs coating on the silk surface, which is important for the subsequent LbL self-assembly process.

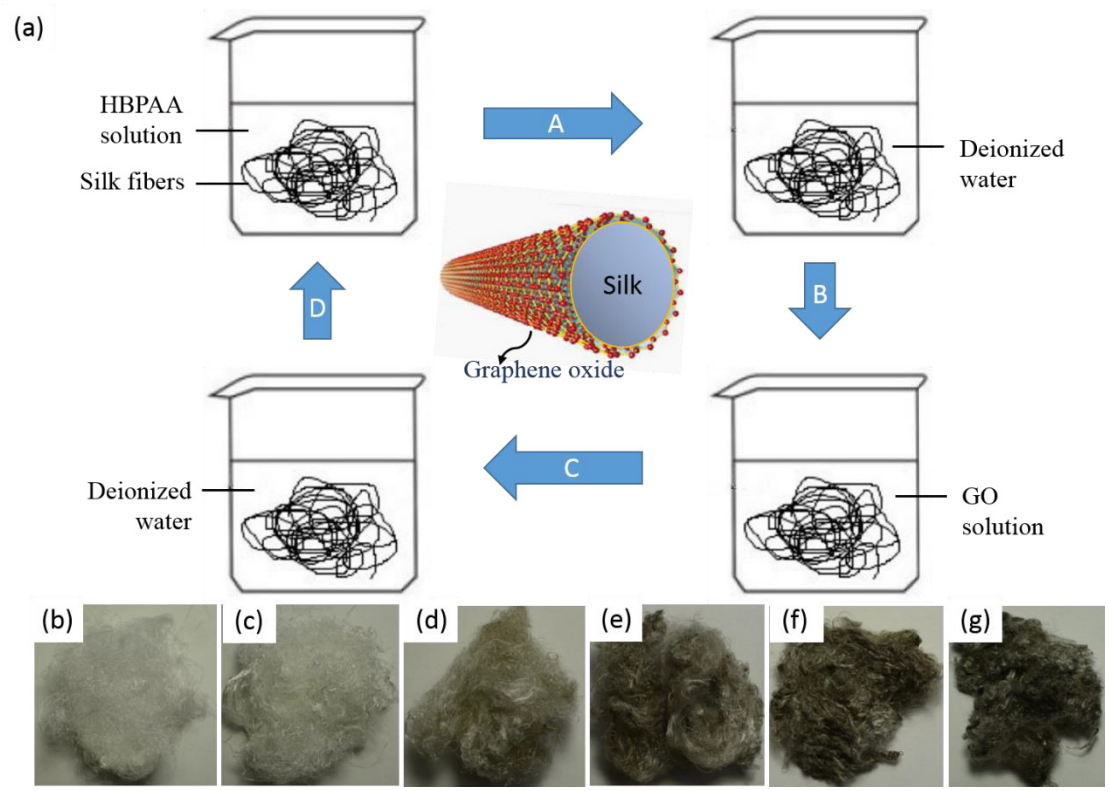

Figure 2. 2 (a) Steps involved in fabrication of GOs /HBPAA -coated silk fibers by LbL self-assembly. The photos of (b) silk fibers, (c) HBPAA-coated silk fibers, and silk fibers treated with (d) one circle, (e) 3 circles, (f) 5 circles and (g) 10 circles.

Specifically, GO-coated silk fibers were constructed by cycle impregnation of silk fibers in solutions of HBPAA and GO. Prior to the design of LBL self-assembly, one important principle needs to declare: GOs should be completely assembled on the surface of silk fibers, with aiming to make full utilization of GOs. The employment of HBPAA as a mediator plays an important role in the assembly process not only because of its cationic characteristic but also their enhanced intermolecular interactions towards silk fibers and GO due to its three-dimensional structure, dense amino end groups, and low viscosity. Therefore, the HBPAA-mediated self-assembly showed much greater loading efficiency than that of cationic linear macromolecules. This advantage makes highly efficient and complete attachment of GOs possible.

As a demonstration, the typical steps involved in the LbL self-assembly of GOs on silk fibers were exhibited in **Figure 2.2 a.** Briefly, silk fibers were first immersed in the solution of HBPAA at 70 ^{o}C for 1 h contact time. HBPAA-coated silk fibers were then dipped in GOs solution and stirring for 1 min. After black color of GOs disappeared, the GO-coated silk fibers were washed with deionized water and in turn immersed into HBPAA solution at room temperature. The density of GOs coating can be controlled by repeated circle impregnation. Notably, GOs can be completely adsorbed onto silk fibers in each circle, ensuring their high production and economic efficiency. **Figure 2.2 b - g** showed the photos of (b) silk fibers, (c) HBPAA-coated silk fibers, and silk fibers after treated with (d) one circle, (e) 3 circles, (f) 5 circles and (g) 10 circles LbL self-assembly.

2.3.3. FTIR analysis

FTIR measurement was applied to evidence the anchor of HBPAA to silk fibers. **Figure 2.3** showed the FTIR spectra of silk fibers and HBPAA-coated silk fibers treated with ten cycles. In the case of pure silk, curve a showed typical adsorption bands of silk protein including CH_2 asymmetric and symmetric stretching vibrations at 2924 and 2850 cm^{-1}, amide I ranged in 1700-1550 cm^{-1}, and amide II ranged in 1550-1450 cm^{-1}.

After ten circles treatment, the weak absorption peaks of CH_2 asymmetric and symmetric stretching vibrations and amino III region were both strengthened, owing to the overlay effect of absorption bands of C-H vibrations and amino III from HBPAA. The phenomenon of the transfer of GOs from the liquid phase to the surface of silk fibers could be observed directly.

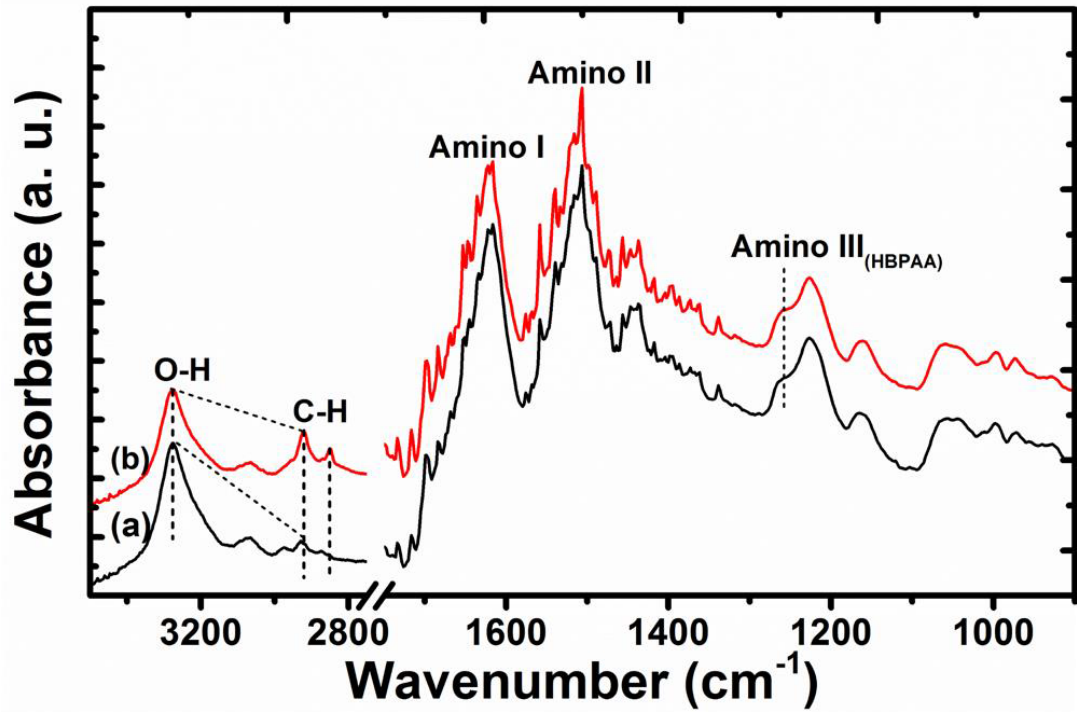

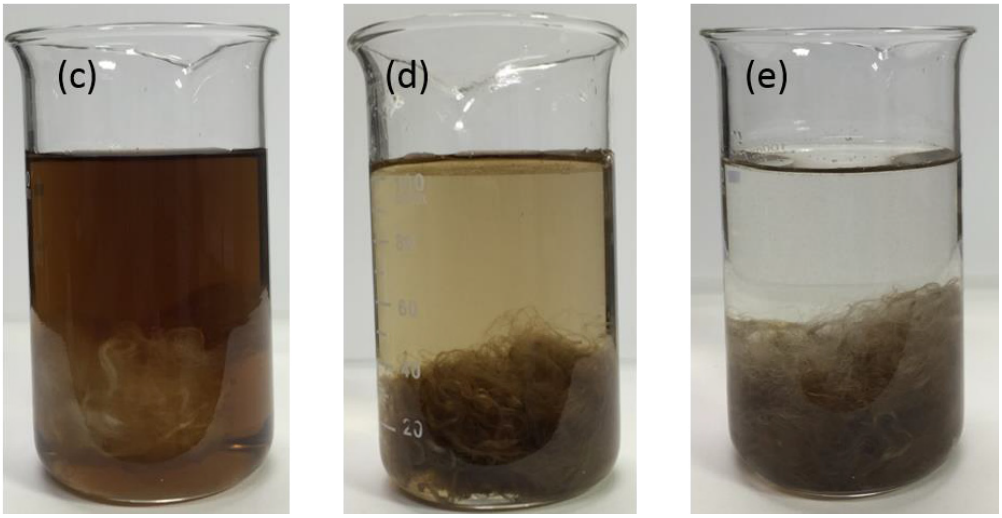

Figure 2. 3 FTIR of (a) pristine silk fibers and (b) GOs /HBPAA coated silk fibers for ten circles LbL assembly, the photographs of the GOs solution and HBPAA coated silk fibers in one cycle LbL assembly under the stirring for (c) 0, (d) 1 and (e) 10 min, respectively.

Figure 2.3 c - e showed the typical photographs of the GOs solution and silk fibers in one cycle LbL assembly under the stirring for 0, 1 and 10 min, respectively. The characteristic brown color of GOs faded gradually in the solution accompanying gradually darken silk fibers during the LbL self-assembly process and finally, the solution of GOs became completely colorless transparent, confirming that GOs in the colloidal solution was coated on the HBPAA-coated silk fibers. Notably, since GOs could be completely adsorbed by silk fibers in each cycle, the precise adjustment of the adsorbed dose of the GOs could be achieved by design the cycle index of the LbL self-assembly.

2.3.4. FESEM analysis

The surface morphology of the silk fibers, particularly the dispersion state of GOs, was observed by FESEM. **Figure 2.4** showed FESEM photographs of the pristine silk fiber, GOs/HBPAA coated silk fibers for one and ten circles treatments. Pure silk fibers exhibited a clean but a little-rugged surface (**Figure 2.4a**). With one circle treatment, GOs/HBPAA coated silk fibers showed the distinct surface pattern to their pristine silk fibers. Although it is difficult to observe the whole morphology of the GOs, numerous small wrinkles that were different from the surface texture of silk and a fraction of large buckling deformation were clearly visible, mainly caused by the crimp or warping of GO nanosheets (**Figure 2.4b**).

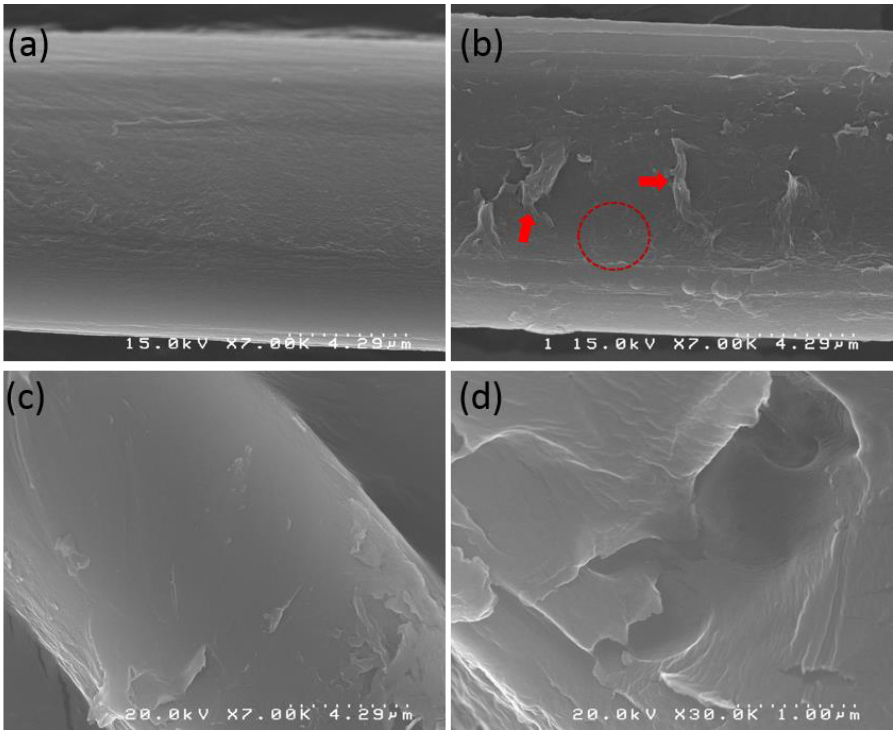

Figure 2. 4 FESEM photographs of the (a×7,000) pristine silk fibers and the GOs/HBPAA coated silk fibers with one circle (b×7,000) and ten circles treatment (c×7,000, d×30,000).

Interestingly, except for a small part of large warps, GOs seem to be closely attached and monodispersed onto silk surface since the surface texture of silk can be clearly seen through these GO films. This indicates that GOs may keep their original thickness and were without serious accumulation, mainly attributing to their flexibility and strong electrostatic repulsion. After ten circles treatment, a multilayered GO films were found and their coating appeared much more stiffness compared to that treated with one circle as shown in **Figure 2.4c and d**. Nevertheless, GOs were found to well adhere to silk fibers although a fraction of upwarping zones was observed, which should be owed to strong electrostatic attraction and hydrogen bonding interactions between GOs and HBPAAs. The close attachment of GOs on silk surface is very important. The large contact area could enhance their adhesion strength with the final improvement of abrasive resistance of GO coating. In summary, GOs were closely attached on the silk surface though some warping of GOs existed.

2.3.5 TGA analysis

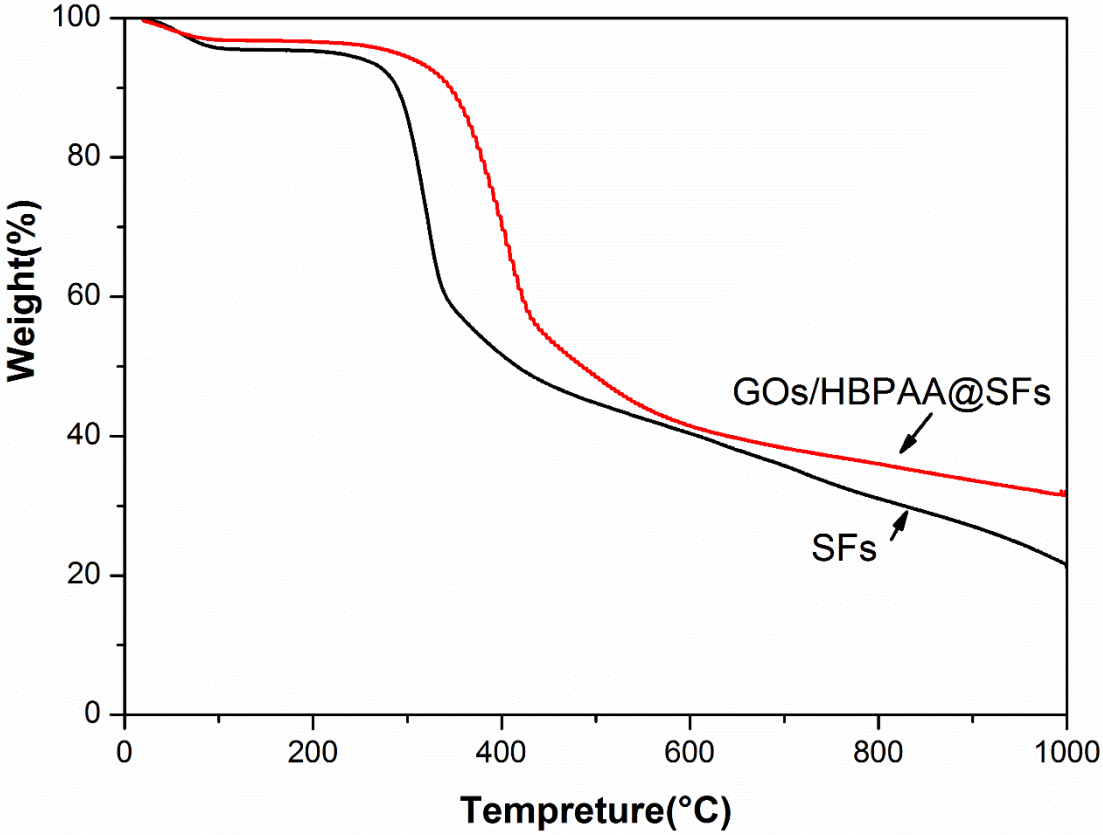

Figure 2. 5 A Comparison of the thermogravimetric curves of silk fibers, SFs, and GOs/HBPAA coated silk fibers (GOs/HBPAA @SFs) treated with ten cycles.

The thermal properties of two silk fibers were compared by TGA by increasing the temperature from 20 to 1000°C in a nitrogen atmosphere. The recorded TG curves were shown in **Figure 2.5**, where both silk fibers have about 4% moisture which was fast removed during the initial temperature increase stage, e.g. from 20 to 100°C. According to **Figure 2.5**, the normal silk fiber has a degradation temperature at about 167°C, and this temperature would be enhanced to about 228°C for the GOs/HBPAA-coated silk fibers (GOs/HBPAA @SFs) treated with ten cycles. This finding has not only again proven the presence of GOs/HBPAA on silk fibers but also importantly indicated that the GOs/HBPAA @SFs can enhance the thermal stability of silk fibers.

2.3.6. XPS analysis

The surface composition of GOs/HBPAA coated silk fibers were measured by XPS (**Figure 2.6**). Silk fibers mainly consist of glycine residues alternating with alanine and serine in the crystalline region, whereas the sequence in the amorphous region contains a tyrosine-rich domain. Thus, silk fibers are considered to mainly contain carbon (C), oxygen (O), and nitrogen (N), in line with the measurement from the wide-scan XPS spectra of silk fibers (red line in **Figure 2.6a**). Conversely, GOs are a one-atom-thick two-dimensional plane of sp^2-bonded carbon with a small quantity of epoxy groups spread across the basal planes and hydroxyl and carboxyl end groups in the peripheries of the plane, with main composition component of C and the small amount of O[35]. Therefore, after coating GOs on silk fibers, the relative ratios of C, O, N elements in GOs/HBPAA coated silk fibers will change. As shown in **Figure 2.6a**, in comparison with pristine silk, the ratio of C/O greatly increased while O/N seemed to remain about the same, contributing to the attachment of GOs on the surface of silk fibers because of the much higher content of C element in GOs. Besides, because GO nanosheets do not contain N element, the O/N ratio showed no obvious change. The presence of GOs on silk fibers can also be evidenced by the photoelectron lines of C1s XPS of silk fibers and GOs/HBPAA coated silk fibers. The main carbon functional structures of silk fibers can be deconvoluted to three major peaks including C=C/C-C, C=O (amide), and C-O (epoxy and alkoxy) (**Figure 2.6a**) [36]. After coating GOs, changes of their related proportion appeared. As displayed in **Figure 2.6b**, the proportion of C-O increased while that of C=O decreased. Considering that GOs have much higher content of C-O bond compared to silk, above changes should be attributed to the attachment of GOs on the surface of silk [37].

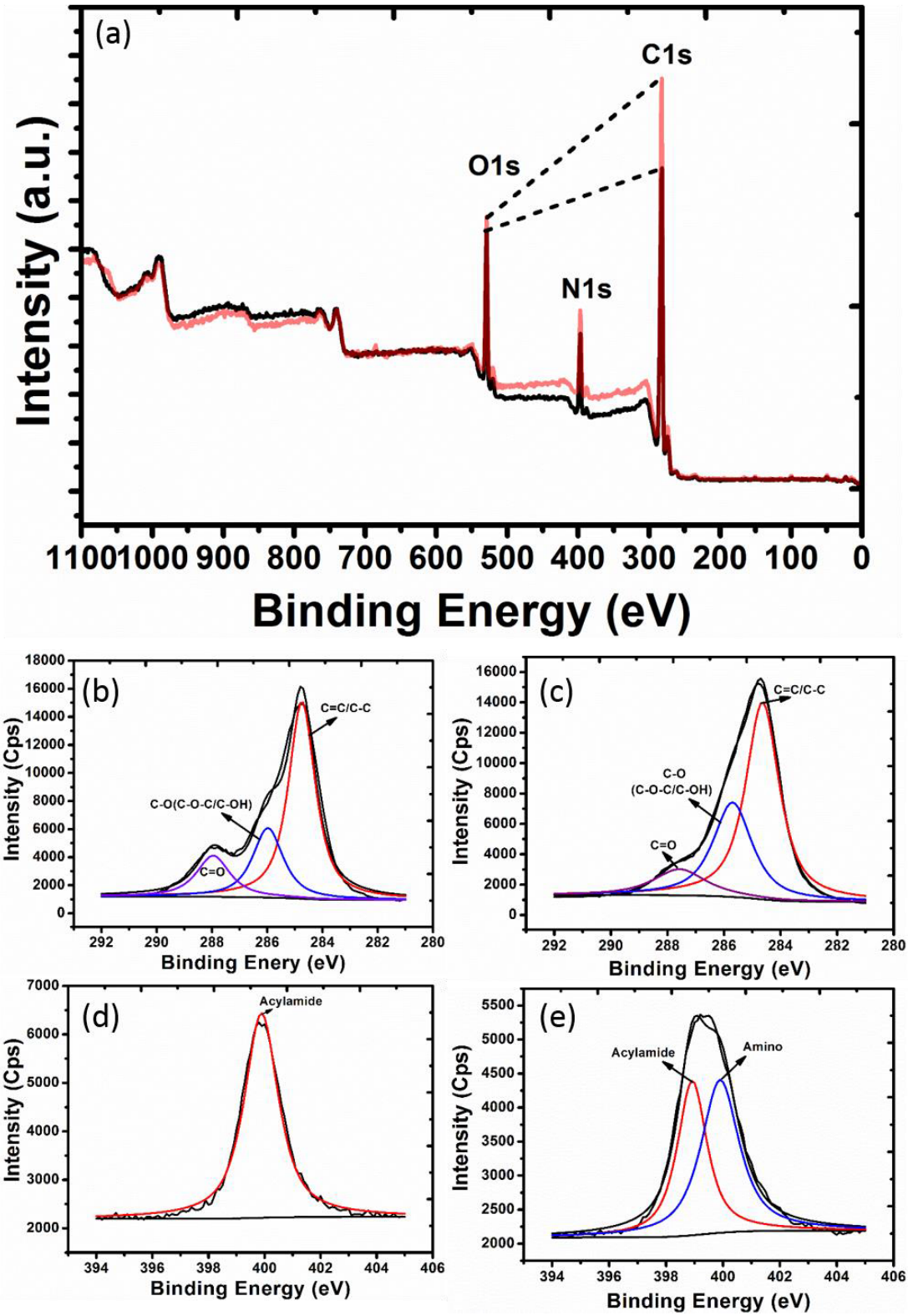

Figure 2. 6 XPS spectra: (a) wide scan spectra of pristine silk fibers (black) and GOs/HBPAA coated silk fibers for ten circles treatment (red) and (b) Related N1s and C1s spectra of (b, d) pristine silk fibers and (c, e) GOs /HBPAA coated silk fibers (ten cycles).

Interestingly, the attachment of HBPAAs on silk fibers can be evidenced from the curve fitting of N1s peaks of XPS spectra. Since GOs is an N-free carbon material, the chemical transformation of N element in GOs/HBPAA coated silk fibers can be responsible to HBPAAs. Besides, although HBPAAs show similar chemical composition to silk macromolecules, the related ratio of amino and acylamide groups were distinct. Silk mainly contains acylamide groups while amino groups dominate in HBPAAs, meaning the relative content of amino groups in HBPAAs is much higher than in silk. **Figure 2.6 d - e** showed the fitting curves of the N1s XPS spectra of silk fibers and GOs/HBPAA coated silk fibers. As amino and acylamide groups are main functional groups of nitrogen in the silk and HBPAA. The N1s peak could be deconvoluted into two component peaks corresponding to amino and acylamide nitrogen at 398.5 eV and 399.8 eV, respectively. In the case of silk, the N element mainly exists in acylamide and amino groups was not found. However, in the case of GOs/HBPAA coated silk fibers, the N1s peak greatly broadened and the relative proportion of amino groups greatly increased, almost same to that of acylamide, indicating that amino-terminated HBPAAs have been anchored to the surface of silk fibers.

2.4. Conclusions

In the study, the tightly-adhered GOs coatings were achieved by a LbL assembly method with solutions of HBPAA and GOs, which HBPAA served as the “molecular glue”. FTIR, FESEM, and XPS were used to characterize the as-prepared GO-coated silk fibers. The FTIR measurement showed that absorption peaks of CH_2 asymmetric and symmetric stretching vibrations and amino III region both strengthened, indicating attachment of HBPAA. FESEM indicated that GOs were well spread on the silk surface and were no serious stacking even after ten cycle treatments. Wide-scan, C1s, and N1s XPS analysis further confirmed the attachment of HBPAA and GOs. In the experiment, GOs were able to completely adsorb onto silk fibers, indicating our LbL self-assembly

technology was efficient and what's more, the GO content in silk fibers could increase with the coating cycle which makes the GO content is easier to be controlled. And this method can be applied as the templates for the control synthesis of GOs coated silk fiber. The GOs coated silk fiber prepared in this study may have potential in the application of medical material and electron device.

References

[1] Hashimoto T, Taniguchi Y, Kameda T, Tamada Y, Kurosu H. Changes in the properties and protein structure of silk fibroin molecules in autoclaved fabrics. Polymer Degradation & Stability. 2015;112:20-6.

[2] Shang S, Zhu L, Fan J. Physical properties of silk fibroin/cellulose blend films regenerated from the hydrophilic ionic liquid. Carbohydrate Polymers. 2011;86:462-8.

[3] Zhong J, Liu X, Wei D, Yan J, Wang P, Sun G, et al. Effect of incubation temperature on the self-assembly of regenerated silk fibroin: a study using AFM. International Journal of Biological Macromolecules. 2015;76:195-202.

[4] Zhang W, Zhang D, Chen Y, Lin H. Hyperbranched polymer functional TiO 2 nanoparticles: Synthesis and its application for the anti-UV finishing of silk fabric. Fibers & Polymers. 2015;16:503-9.

[5] Xu S, Chen S, Zhang F, Jiao C, Song J, Chen Y, et al. Preparation and controlled coating of hydroxyl-modified silver nanoparticles on silk fibers through intermolecular interaction-induced self-assembly. Materials & Design. 2016;95:107-18.

[6] Song J, Xu S, Chen T, Morikawa H. Fabrication of hierarchical structured graphene oxide-Fe3O4 hybrid nanosheets and Ag nanoparticles bimetallic composite coated silk fibers through self-assembly. 2017:59-68.

[7] Xu S, Song J, Morikawa H, Chen Y, Lin H. Fabrication of hierarchical structured Fe 3 O 4 and Ag nanoparticles dual-coated silk fibers through electrostatic self-assembly. Materials Letters. 2016;164:274-7.

[8] Geim AK, Novoselov KS. The rise of graphene. Nat Mater. 2007;6:183-91.

[9] Paredes JI, Villar-Rodil S, Fernandez-Merino MJ, Guardia L, Martinez-Alonso A, Tascon JMD. Environmentally friendly approaches toward the mass production of processable graphene from graphite oxide. Journal of Materials Chemistry.

2011;21:298-306.

[10] Hu K, Gupta MK, Kulkarni DD, Tsukruk VV. Ultra-Robust Graphene Oxide-Silk Fibroin Nanocomposite Membranes. Advanced Materials. 2013;25:2301-7.

[11] Li J-L, Tang B, Yuan B, Sun L, Wang X-G. A review of optical imaging and therapy using nanosized graphene and graphene oxide. Biomaterials. 2013;34:9519-34.

[12] Georgakilas V, Tiwari JN, Kemp KC, Perman JA, Bourlinos AB, Kim KS, et al. Noncovalent Functionalization of Graphene and Graphene Oxide for Energy Materials, Biosensing, Catalytic, and Biomedical Applications. Chemical Reviews. 2016.

[13] Seah C-M, Vigolo B, Chai S-P, Mohamed AR. Mechanisms of graphene fabrication through plasma-induced layer-by-layer thinning. Carbon. 2016;105:496-509.

[14] Shan C, Yang H, Han D, Zhang Q, Ivaska A, Niu L. Water-soluble graphene covalently functionalized by biocompatible poly-L-lysine. Langmuir. 2009;25:12030-3.

[15] Ma J, Zhang J, Xiong Z, Yong Y, Zhao X. Preparation, characterization and antibacterial properties of silver-modified graphene oxide. Journal of Materials Chemistry. 2011;21:3350-2.

[16] Georgakilas V, Otyepka M, Bourlinos AB, Chandra V, Kim N, Kemp KC, et al. Functionalization of Graphene: Covalent and Non-Covalent Approaches, Derivatives and Applications. Chemical Reviews. 2012;112:6156-214.

[17] Qu Y, Ma M, Wang Z, Zhan G, Li B, Wang X, et al. Sensitive amperometric biosensor for phenolic compounds based on graphene–silk peptide/tyrosinase composite nanointerface. Biosensors and Bioelectronics. 2013;44:85-8.

[18] Maktedar SS, Mehetre SS, Singh M, Kale R. Ultrasound irradiation: A robust approach for direct functionalization of graphene oxide with thermal and antimicrobial aspects. Ultrasonics sonochemistry. 2014;21:1407-16.

[19] Suresh I, Chidambaram K, Vinod V, Rajender N, Venkateswara RM, Miroslav Č.

Synthesis, characterization and optical properties of graphene oxide–polystyrene nanocomposites. Polymers for Advanced Technologies. 2015;26:214-22.

[20] Cong H-P, Ren X-C, Wang P, Yu S-H. Macroscopic Multifunctional Graphene-Based Hydrogels and Aerogels by a Metal Ion Induced Self-Assembly Process. ACS Nano. 2012;6:2693-703.

[21] Valentini L. Bio-inspired materials and graphene for electronic applications. Materials Letters. 2015;148:204-7.

[22] Akhavan O, Ghaderi E. Toxicity of graphene and graphene oxide nanowalls against bacteria. ACS nano. 2010;4:5731-6.

[23] Hu W, Peng C, Luo W, Lv M, Li X, Li D, et al. Graphene-based antibacterial paper. Acs Nano. 2010;4:4317-23.

[24] Liu S, Zeng TH, Hofmann M, Burcombe E, Wei J, Jiang R, et al. Antibacterial Activity of Graphite, Graphite Oxide, Graphene Oxide, and Reduced Graphene Oxide: Membrane and Oxidative Stress. ACS Nano. 2011;5:6971-80.

[25] Zhao J, Deng B, Lv M, Li J, Zhang Y, Jiang H, et al. Graphene Oxide-Based Antibacterial Cotton Fabrics. Advanced Healthcare Materials. 2013;2:1259-66.

[26] Moon IK, Lee J, Ruoff RS, Lee H. Reduced graphene oxide by chemical graphitization. Nature communications. 2010;1:73.

[27] Maddinedi SB, Mandal BK, Vankayala R, Kalluru P, Pamanji SR. Bioinspired reduced graphene oxide nanosheets using Terminalia chebula seeds extract. Spectrochimica Acta Part A: Molecular and Biomolecular Spectroscopy. 2015;145:117-24.

[28] Aghigh A, Alizadeh V, Wong H, Islam MS, Amin N, Zaman M. Recent advances in utilization of graphene for filtration and desalination of water: A review. Desalination. 2015;365:389-97.

[29] Akhavan O, Azimirad R, Gholizadeh H, Ghorbani F. Hydrogen-rich water for green reduction of graphene oxide suspensions. International Journal of Hydrogen Energy. 2015;40:5553-60.

[30] Shen J, Hu Y, Li C, Qin C, Shi M, Ye M. Layer-by-layer self-assembly of graphene nanoplatelets. Langmuir. 2009;25:6122-8.

[31] Xu S, Chen S, Zhang F, Jiao C, Song J, Chen Y, et al. Preparation and controlled coating of hydroxyl-modified silver nanoparticles on silk fibers through intermolecular interaction-induced self-assembly. Materials & Design. 2016.

[32] Tung VC, Allen MJ, Yang Y, Kaner RB. High-throughput solution processing of large-scale graphene. Nature nanotechnology. 2009;4:25-9.

[33] Chen J, Yao B, Li C, Shi G. An improved Hummers method for eco-friendly synthesis of graphene oxide. Carbon. 2013;64:225-9.

[34] Shahriary L, Athawale AA. Graphene oxide synthesized by using modified hummers approach. IJREEE. 2014;2:58-63.

[35] Li W, Geng X, Guo Y, Rong J, Gong Y, Wu L, et al. Reduced Graphene Oxide Electrically Contacted Graphene Sensor for Highly Sensitive Nitric Oxide Detection. ACS Nano. 2011;5:6955-61.

[36] Chen G, Zhou M, Zhang Z, Lv G, Massey S, Smith W, et al. Acrylic Acid Polymer Coatings on Silk Fibers by Room-temperature APGD Plasma Jets. Plasma Processes and Polymers. 2011;8:701-8.

[37] Zhang J, Yang H, Shen G, Cheng P, Zhang J, Guo S. Reduction of graphene oxide vial-ascorbic acid. Chemical Communications. 2010;46:1112-4.

Chapter 3: Graphene oxide-encapsulated Ag nanoparticle-coated silk fibers with hierarchical coaxial cable structure fabricated by the molecule-directed self-assembly

Chapter 3 Graphene oxide-encapsulated Ag nanoparticle-coated silk fibers with hierarchical coaxial cable structure fabricated by the molecule-directed self-assembly

3.1 Introduction

Bombyx mori silk, a protein fiber derived from *Bombyx mori* silkworm cocoons, is known to be one of the strongest natural biomaterials [1]. Different from cotton and wool containing various substances, silk fibers were mainly composed of long-chain polypeptides. Sericin is an amorphous protein that can be removed by the degumming process. Silk fibroin is composed of numerous minute fibrils, which could be separated into β-sheet crystals with strong hydrogen bonding and a non-crystalline (amorphous) region with varying degrees of hydrogen bonding[2]. The amino-acid sequence in the crystalline region of the silk fibroin is mainly composed of glycine residues alternating with alanine and serine and the sequence in the amorphous region contains a tyrosine-rich domain.[3, 4] Silk fibroin fibers gain smooth and clear surfaces with good chemical activity, which can be easily combined with other functional materials [5-7]. One interest subject is coating inorganic materials to silk fibroin fibers to create multiscale composite materials for medical applications.

Inorganic nanoparticles (NPs) have emerged as indispensable building blocks for various functional biomaterials owing to their unique physico-chemical properties that can extend the applicability of traditional biomaterials to various fields such as biomedicine, drug delivery, biosensors, and wearable devices [8, 9]. However, their potential in nanocoatings on natural fibers remains somehow underestimated because of same weaknesses such as low adhesion strength, uncontrollable spatial arrangement of NPs, and the lack of biocompatibility. Besides, because NPs coatings are exposed to the external complex physical and chemical environment, a function decrease under persistent external stimuli such as sunlight radiation, mechanical friction, and chemical

action (e.g., oxidation and chlorination) is inevitable during use. In the electrical industry, cables were usually designed to a coaxial structure to protect the internal metallic wires from corrosion. Inspired by this, we plan to encapsulate nanocoatings by a robust protective layer possessing higher chemical and thermodynamic stability and better mechanical properties. GO nanosheets are surely the most ideal candidate in the present study because of their extraordinary chemical, mechanical, optical, and thermal properties [10].

In this study, we demonstrated GO-encapsulated AgNP-coated silk fibers through molecule-directed self-assembly. To construct a hierarchical structure, a stepwise colloidal self-assembly technology was developed by successively impregnating silk fibers with HBPAA/AgNPs and GOs. HBPAA capping on the AgNP surfaces were served as an effective "adhesive glue", not only directing AgNPs to silk surfaces to form a stable, uniform, and mono-dispersed nanocoatings but also attracting GOs to the AgNP surfaces and forming a closely bonded sandwich structure. Notably, GOs were reported to have high antibacterial activities against various bacteria [11]. Therefore, the GO-encapsulated AgNP-coated silk fibers were supposed to gain synergic antibacterial effects. In addition, by encapsulating AgNPs in metal-free GO films, AgNPs were isolated from the human body, which may improve the biosecurity.

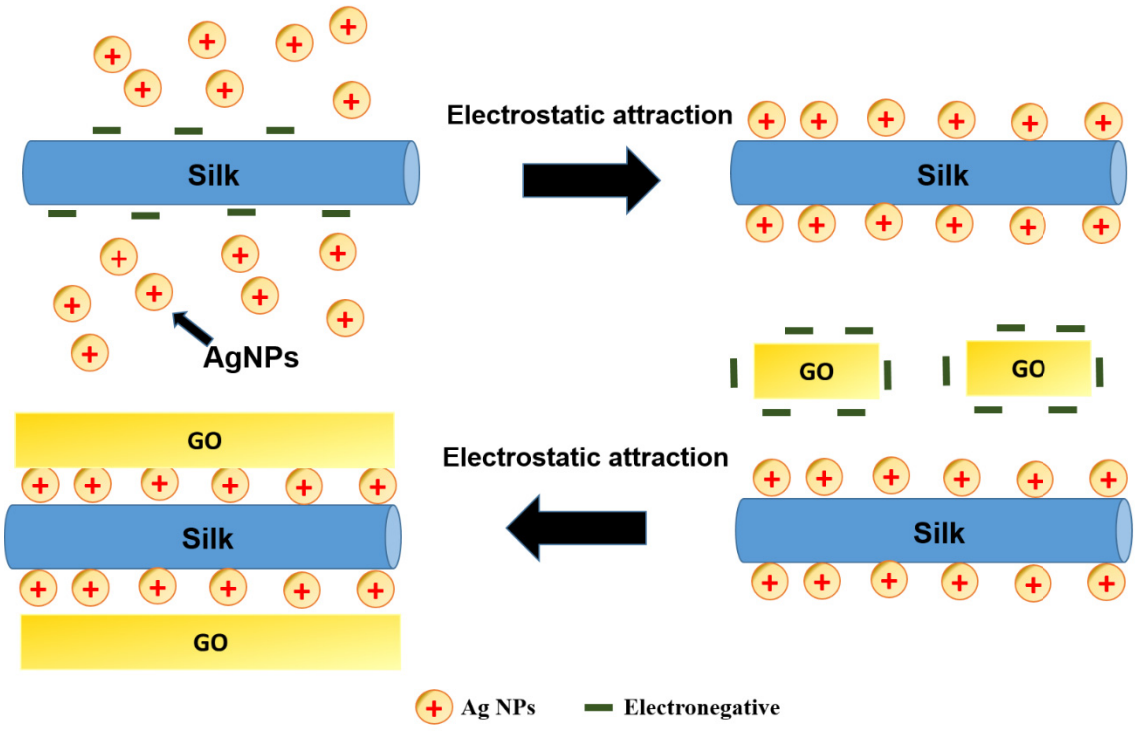

Figure 3. 1 Schematic representation of the colloidal self-assembly procedure of GO-encapsulated AgNP-coated silk fibers.

3.2 Experimental

3.2.1 Preparation of GO-encapsulated AgNP-coated silk fibers by HBPAA-directed self-assembly

GOs and HBPAA/AgNPs were prepared by our reported method [12, 13].Two grams of SFs was first immersed into a beaker containing 100 mL of 10 g/L HBPAA solution at 98 °C. After 1 h of contact time, SFs were removed from the solution and rinsed thoroughly with water to remove unattached HBPAA. Silk fibers were immersed into a 100 mL of 1.5 mg/mL aqueous solution of HBPAA/AgNPs. By keeping stirring at 95 °C for 2 h, as-prepared AgNP-coated fibers were rinsed in deionized water three times and dried in an oven at 90 ^{o}C. Subsequently, coated fibers were impregnated with 100 mL of GO colloid solution (1.5 mg/mL, pH=6.3) and kept stirring at 90 °C for 3 h. Finally, the resulting samples were rinsed with deionized water, cured in an oven at 120 ^{o}C, and encapsulated in sample bags.

3.2.2 Measurements

The morphology and crystal structure of HBPAA/AgNPs were investigated using a transmission electron microscope (TEM) (S-4800; Hitachi, Japan) operating at an accelerating voltage of 120 kV. The morphology and size of the composite SFs were observed using a field-emission scanning electron microscope (FESEM) (S4800; Hitachi, Japan). The surface chemical structure of the GOs, silk fibers, HBPAA/AgNP-coated silk fibers, and GO-encapsulated AgNP-coated silk fibers were characterized by X-ray photoelectron spectroscopy (XPS) using an X-ray diffractometer (Krotos, Japan, AXIS Ultra DLD). The crystal structure of pristine and modified SFs was examined by an X-ray diffractometer (XRD) (D8 ADVANCE, Bruker, Germany).

3.3 Results and discussion

3.3.1 Characterization of GOs and as-prepared HBPAA/AgNPs

In this work, GO sheets were prepared by the oxidation and exfoliation of nature graphite in the aqueous solutions using a modified Hummer' method. As shown in Figures 3.2 a and b, as-prepared GO showed a film-like morphology. The height difference between two red short dashes is around 1 nm, indicative of a one-atom-thick GO sheet. HBPAA/AgNPs were prepared through reduction of silver nitrate by HBPAA in the aqueous solution. As-prepared AgNPs exhibited a uniform particle size with the mean grain size of around 10.5 nm and good crystallinity (Figures 3.2 c and d).

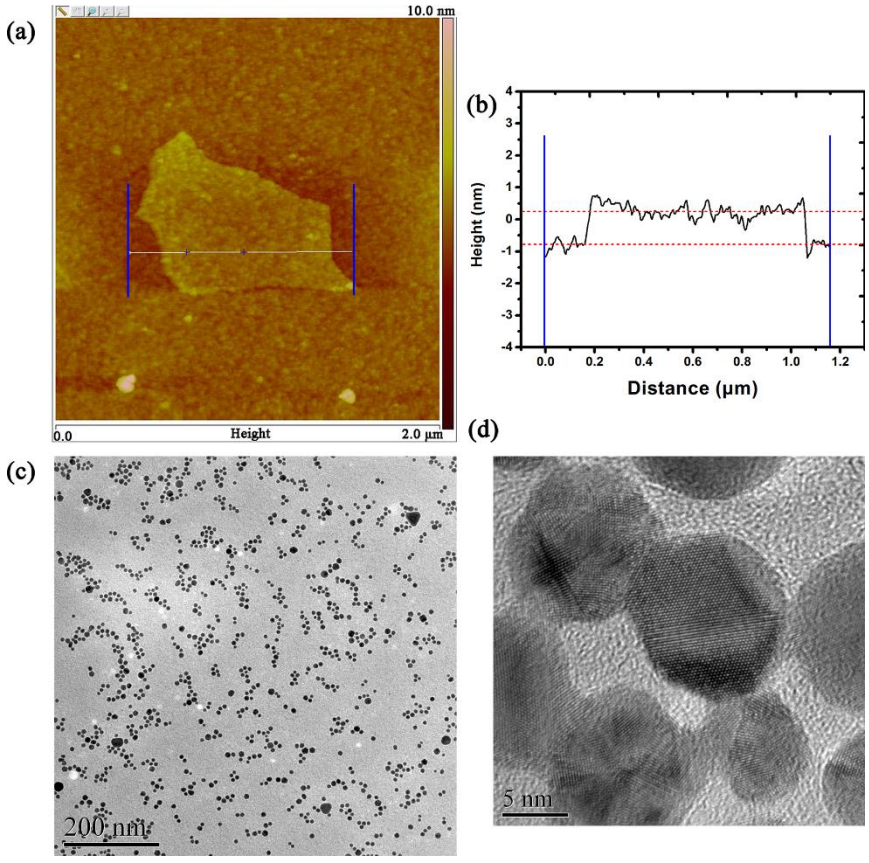

Figure 3. 2 (a, b) AFM image of a typical GO sheet deposited on silicon and the corresponding height profiles; (c) TEM and (d) high-resolution TEM of as-prepared HBPAA/AgNPs.

3.3.2 GO-encapsulated AgNP-coated silk fibers through self-assembly

The self-assembly approach to generate hybrid silk is sketched in Figure 3.3. Before starting the assembly procedure, silk fibers were degummed to remove the soluble sericin. Cleaning the silk fiber surfaces was necessary because sericin on the silk surfaces is incompetent to support HBPAA/AgNPs (pH>7.8 in aqueous solution) and GOs due to its high solubility in alkaline solution. The obtained silk fibroin fibers were then transferred to a colloidal solution of HBPAA/AgNPs. By heating the mixture, the HBPAA could transport AgNPs to silk fibroin surfaces by intermolecular interactions between HBPAA and silk fibroin macromolecules. The AgNPs tended to form monolayer coatings because of the electrostatic repulsion among positively charged AgNPs. Besides, HBPAA/AgNPs could be nearly completely adsorbed by silk as shown in Figure 3. Therefore, AgNP density on the silk surfaces could be controlled through adjusting the AgNP concentration. As such, functions of AgNP coatings such as the antibacterial activities and surface plasmon resonance (SPR) would be tunable. The subsequent assembly of GOs to AgNP surfaces was carried out by impregnating AgNP-coated silk fibers in GOs solution. HBPAA attached on AgNP surfaces could attract negatively charged GOs and form a stable hierarchical structure through amino-carboxyl interactions.

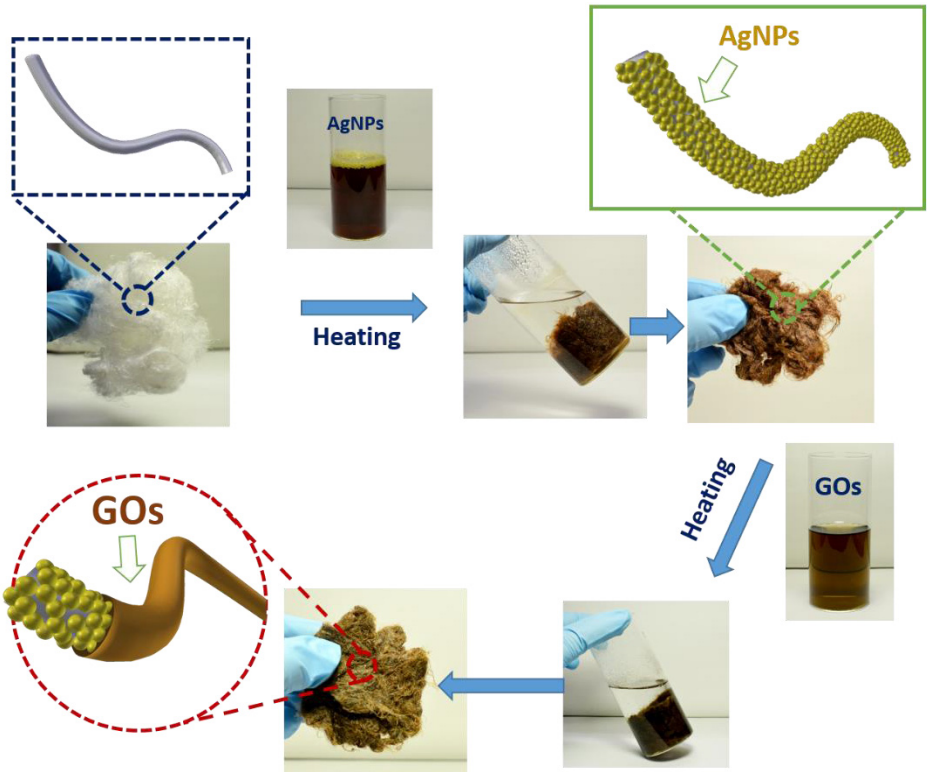

Figure 3. 3 Schematic representation of the colloidal self-assembly procedure of GO-encapsulated AgNP-coated silk fibers.

3.3.3 FESEM analysis

The coaxial cable structure of ternary hybrid fiber composites were confirmed by FESEM. As shown in Figures 3.4 a -d, the clean and smooth surfaces of silk fibers were captured by dense mono-dispersed nanoparticles after self-assembly of HBPAA/AgNPs to the silk surface. For the GO encapsulated sample, spatial arrangement of GOs on the silk could be divide into two aggregation forms. GO nanosheets tend to closely adhere to the fiber surface and form continuous film-like protective layers (Figures 3.4 f and g). Nevertheless, other untrapped GOs were distorted and self-stacked to large bulges as observed in Figure 3.4 e. The hierarchical coaxial cable structure could be evidenced by observing the morphological characteristics of the defect zone of the GO coating. As shown in Figure 3.4 h, numerous nanoparticles were uniformly adhered to the GO-uncovered zone whereas the trace of AgNPs were not found on the GO surfaces, indicating that AgNPs were hidden under the GO multilayers.

Notably, since most silk fiber surface was tightly covered by the robust GO nanosheets owing to strong adhesion strength between carboxyl-containing GOs and amino-functionalized AgNPs, it is expected that HBPAA/AgNPs could be well protected from various external stimuli.

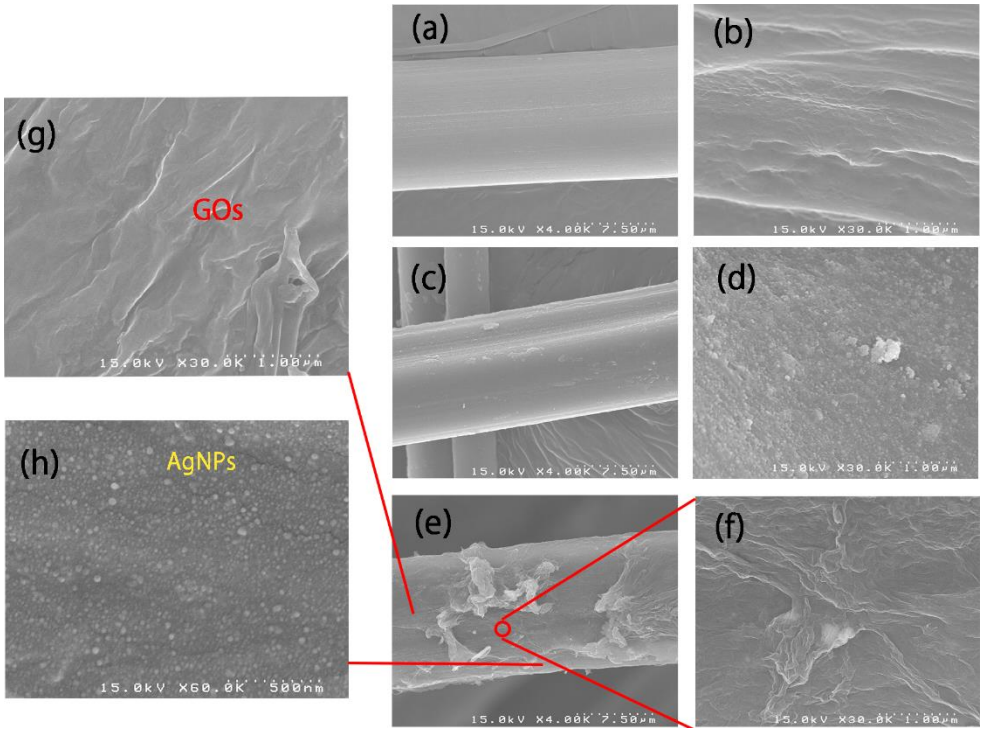

Figure 3. 4 FESEM images of the (a × 4,00K, b × 30,0K) pure silk fiber, (c × 4,00K, d × 30,0K) AgNP-coated silk fiber, and (e × 4,00K, f × 30,0K, g×30.0K, h ×60.0k) GO-encapsulated AgNP-coated silk fiber.

3.3.4 XPS and XRD analysis

The elementary composition and surface chemistry of the silk fiber composites were investigated by XPS (Figure 3.5). All wide-scan XPS spectra showed three ultra-strong peaks located at around 284, 398, and 532 eV, attributed to C1s, N1s, and O1s, respectively. They were mainly derived from silk. In the C1s XPS spectra in Figure 4b, on the basis of the chemical construction of silk, HBPAA, and GOs, C1s peaks can be deconvoluted into four major peaks, that is, C-C/C=C, C-O(H)/C-N, C=O/N-C=O, and O=C-O [14]. After self-assembly of HBPAA/AgNPs to the silk surfaces, the relative intensity of the C-O(H)/C-N bond slightly increased, indicating the successful attachment of amide-rich HBPAA. By contrast, the introduction of GOs to HBPAA/AgNP-coated silk fibers greatly changed the chemical property of silk surfaces. Since GOs contain high content C-O(H), C=O, and O=C-O bonds, the remarkable proportion increase of three oxygen-containing groups in ternary fiber composites suggested large amounts of GOs were assembled to the silk surfaces (see blue line of Figure 3.5). In the Ag3d XPS spectra shown in Figure 4c-4f, the Ag $3d_{3/2}$ and $Ag3d_{5/2}$ peaks of HBPAA/AgNPs-coated silk and GO-encapsulated HBPAA/AgNP-coated silk were both around 374.1 and 368.1 eV, indicating the metallic state of HBPAA/AgNPs [15]. This can also be evidenced by their XRD patterns, in which AgNPs showed the pure face-centered-cubic phase of metallic Ag (JCPDS No. 04-0783) (Figure 3.5 g) [15]. The good chemical stability of AgNP coatings derived from the good protection and high reducibility of HBPAA.

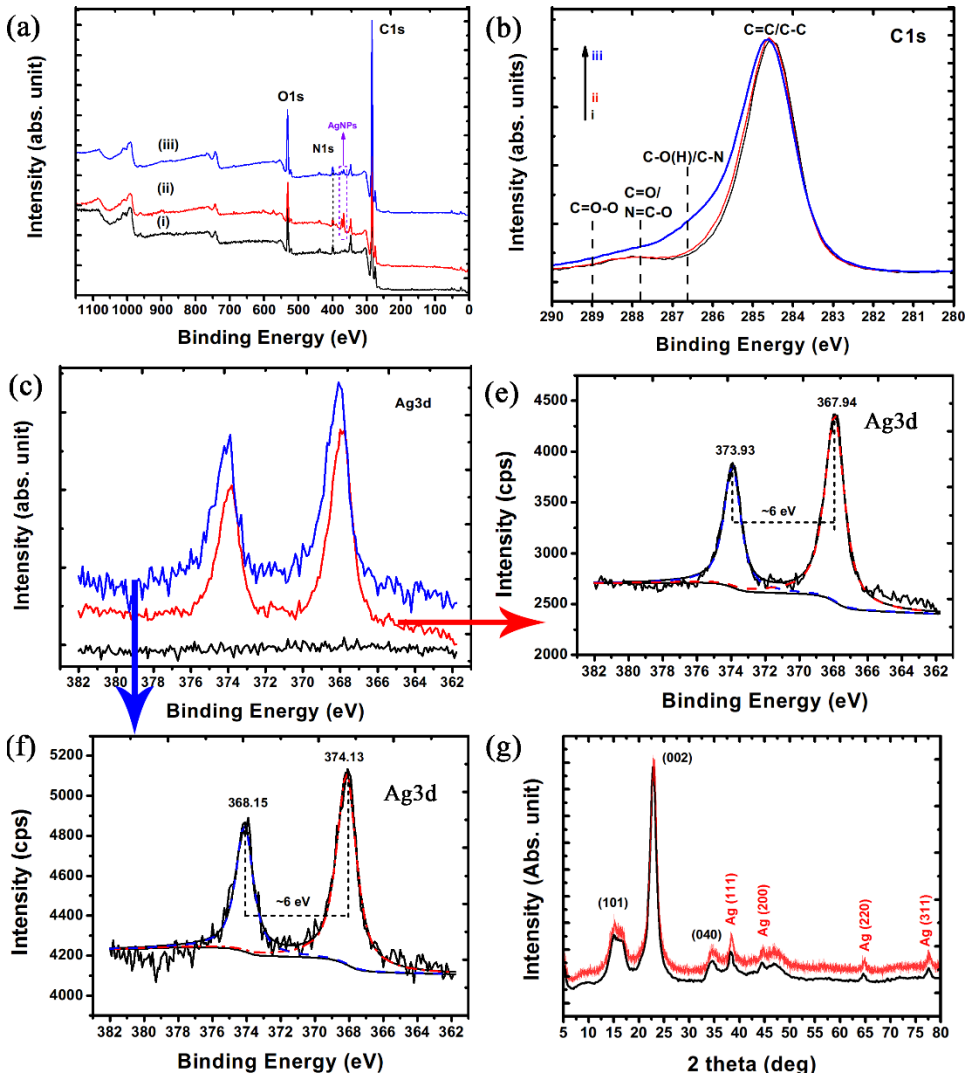

Figure 3. 5 (a) Wide-scan, (b) C1s, and Ag3d (c) XPS spectra and (g) XRD patterns of silk fibers (black), HBPAA/AgNP-coated silk fibers (red), and GO-encapsulated AgNP-coated silk fibers (blue).

3.4 Conclusions

GO-encapsulated AgNP-coated silk fibers with hierarchical coaxial cable structure were successfully fabricated through HBPAA -directed self-assembly. HBPAA was served as a “molecule glue” to adhere GOs, AgNPs, and silk together. The ternary hierarchical structure was constructed by sequentially impregnating silk fibers in solutions of HBPAA/AgNPs and GOs. Our FESEM analysis suggested that the ternary silk composites possessed dense mono-dispersed HBPAA/AgNPs coatings closely encapsulated by GOs. XPS and XRD characterizations showed that large amounts of GOs were successfully coated to metallic AgNP surfaces. The developed coaxial cable structure may provide an effective strategy to protect the functional nanocoatings on the fiber surface.

References

[1] Tao H, Kaplan DL, Omenetto FG. Silk Materials – A Road to Sustainable High Technology. Advanced materials. 2012;24:2824-37.

[2] Tansil NC, Koh LD, Han MY. Functional silk: colored and luminescent. Advanced Materials. 2012;24:1388-97.

[3] Lin N, Meng Z, Toh GW, Zhen Y, Diao Y, Xu H, et al. Engineering of fluorescent emission of silk fibroin composite materials by material assembly. Small. 2015;11:1205-14.

[4] Drummy LF, Phillips DM, Stone MO, Farmer B, Naik RR. Thermally induced α-helix to β-sheet transition in regenerated silk fibers and films. Biomacromolecules. 2005;6:3328-33.

[5] Correia C, Bhumiratana S, Yan L-P, Oliveira AL, Gimble JM, Rockwood D, et al. Development of silk-based scaffolds for tissue engineering of bone from human adipose-derived stem cells. Acta biomaterialia. 2012;8:2483-92.

[6] Kim D-H, Viventi J, Amsden JJ, Xiao J, Vigeland L, Kim Y-S, et al. Dissolvable films of silk fibroin for ultrathin conformal bio-integrated electronics. Nature materials. 2010;9:511-7.

[7] Mou Z-L, Duan L-M, Qi X-N, Zhang Z-Q. Preparation of silk fibroin/collagen/hydroxyapatite composite scaffold by particulate leaching method. Materials Letters. 2013;105:189-91.

[8] Yi F, Wang J, Wang X, Niu S, Li S, Liao Q, et al. Stretchable and Waterproof Self-Charging Power System for Harvesting Energy from Diverse Deformation and Powering Wearable Electronics. ACS nano. 2016;10:6519-25.

[9] Lohse SE, Murphy CJ. Applications of Colloidal Inorganic Nanoparticles: From Medicine to Energy. Journal of the American Chemical Society. 2012;134:15607-20.

[10] Georgakilas V, Tiwari JN, Kemp KC, Perman JA, Bourlinos AB, Kim KS, et al.

Noncovalent Functionalization of Graphene and Graphene Oxide for Energy Materials, Biosensing, Catalytic, and Biomedical Applications. Chemical Reviews. 2016.

[11] Zhao J, Deng B, Lv M, Li J, Zhang Y, Jiang H, et al. Graphene Oxide-Based Antibacterial Cotton Fabrics. Advanced Healthcare Materials. 2013;2:1259-66.

[12] Xu S, Chen S, Zhang F, Jiao C, Song J, Chen Y, et al. Preparation and controlled coating of hydroxyl-modified silver nanoparticles on silk fibers through intermolecular interaction-induced self-assembly. Materials & Design. 2016;95:107-18.

[13] Jiaqing X, Chenlu J, Sijun X, Jin T, Desuo Z, Hong L, et al. Strength-controllable graphene oxide amphiprotic aerogels as highly efficient carrier for anionic and cationic azo molecules. Japanese Journal of Applied Physics. 2015;54:06FF7.

[14] Shao J, Liu J, Zheng J, Carr CM. X-ray photoelectron spectroscopic study of silk fibroin surface. Polymer International. 2002;51:1479-83.

[15] Zhao S, Cheng Z, Kang L, Zhang Y, Zhao X. A novel preparation of porous spong-shaped Ag/ZnO heterostructures and their potent photocatalytic degradation efficiency. Materials Letters. 2016;182:305-8.

Chapter 4: Fabrication of hierarchical structured graphene oxide-Fe_3O_4 hybrid nanosheets and Ag nanoparticles bimetallic coated silk fibers through self-assembly

Chapter 4 Fabrication of hierarchical structured graphene oxide-Fe_3O_4 hybrid nanosheets and Ag nanoparticles bimetallic coated silk fibers through self-assembly

4.1 Intrudction

More and more multi-component nanocomposites include two or more types of nanoparticles and have attracted increasing attention in catalysis, photography, electronic, antibacterial, and optical applications due to their unique functions[1-7]. *Bombyx mori* silk, a protein fiber derived from *Bombyx mori* silkworm cocoons, is known to be one of the strongest natural biomaterials.[8] And because of its good biocompatibility, biodegradation, and friendly environmental performance, silk is an interesting and possible support functional nanoparticles, such as biomaterial for magnetic NPs and antibacterial AgNPs associated with this study. Silk fiber is often used as the first choice for researchers [5, 6, 9, 10]. While Fe_3O_4 and γ-Fe_2O_3 nanoparticles with good biocompatibility and low toxicity can be used for recycling of AgNPs without a decrease in their antibacterial activities. In the specific R & D process, silk fiber as a biomedical material plays a key role in the design and synthesis of nanocomposite materials with controllable loading with nanoparticles dispersed on the surface of the chains. And all of these applications required suitable stabilization of the magnetic nanoparticles to prevent their aggregation and chemical transformation. The usual route is chosen in situ preparation of Fe_3O_4 and AgNPs using silk fiber as a bio-template, which is hard to prevent aggregation of Fe_3O_4NPs and chemical transformation of AgNPs[1, 11-15].

Based on our previous studies[6, 10], we also attempted to improve the process and design a new structure for the multifunctional nanocomposite fiber materials. Design and fabrication of well-organized hierarchical structured GO-Fe_3O_4NPs hybrid nanosheets and AgNPs bimetallic composite coated silk fibers to meet multi-functional

requirements via a facile and simple assembly technology remain a significant challenge. We select octadecylamine (ODA) modified graphene to prepare GO-Fe_3O_4 hybrid nanosheets to overcome the above difficulties, because the hydrophobic property of the octadecylamine, the good dispersibility of graphene oxide is obviously improved, which effectively prevent the aggregation of Fe_3O_4NPs, when Fe_3O_4NPs grow on the surface of GO-ODA[3]. In this case, based on our previous studies [10] and the carrier of graphene or graphene oxides and silk fibers, by encapsulating AgNPs in metal-free GO films, AgNPs were isolated from the human body, which may improve the biosecurity to prevent AgNPs from chemical transformation.

Here we prepared novel hierarchical structured GO-Fe_3O_4NPs/AgNPs bimetallic composite coated silk fibers via a special electrostatic self-assembly technology using positively charged AgNPs and negatively charged GO-Fe_3O_4NPs hybrid nanosheets as the building blocks. Specifically, GO-Fe_3O_4NPs/AgNPs bimetallic composite coated silk fibers were facilely obtained by sequential impregnation with solutions of HBPAA-capped AgNPs and citric acid-capped GO-Fe_3O_4NPs hybrid nanosheets.

4.2 Exiperimental

4.2.1 Materials

Silk fibers were obtained from the Ueda Fujimoto Co., Ltd (Japan). HBPAA was synthesized according to our previous research[16]. GOs were synthesized by oxidizing graphite powder using a modified Hummers method [17-19]. Octadecylamine (ODA), $AgNO_3$, and $FeCl_3 \cdot 6H_2O$, $FeCl_2 \cdot 4H_2O$, citric acid and $NH_3 \cdot H_2O$ (25 wt %) were purchased from Wake Pure Chemical Industries CO., LTD... All other reagents were at least of analytical reagent grade and used without further purification. Distilled water was used in all the processes of aqueous solution preparations and washings.

4.2.2 Preparation of GO-Fe_3O_4NPs/AgNPs dual-coated silk fibers by electrostatic assembly

4.2.2.1 Synthesis of positively charged AgNPs

GOs and HBPAA/AgNPs were prepared by our reported method [6, 16, 20]. The mechanism of interaction between Ag NPs and silk fibroin was illustrated in **Figure 4.1**. Positively charged HBPAA-capped AgNPs were synthesized by adding 48 mL of HBPAA solution (0.21 mM) to 2 mL of $AgNO_3$ (46.3 mM) at 35 °C using a well-described procedure. The reaction mixture was slowly heated to 90 °C and kept stirring at 90 °C for 3 h. This resulting solution was dialyzed against distilled water for 72 h.

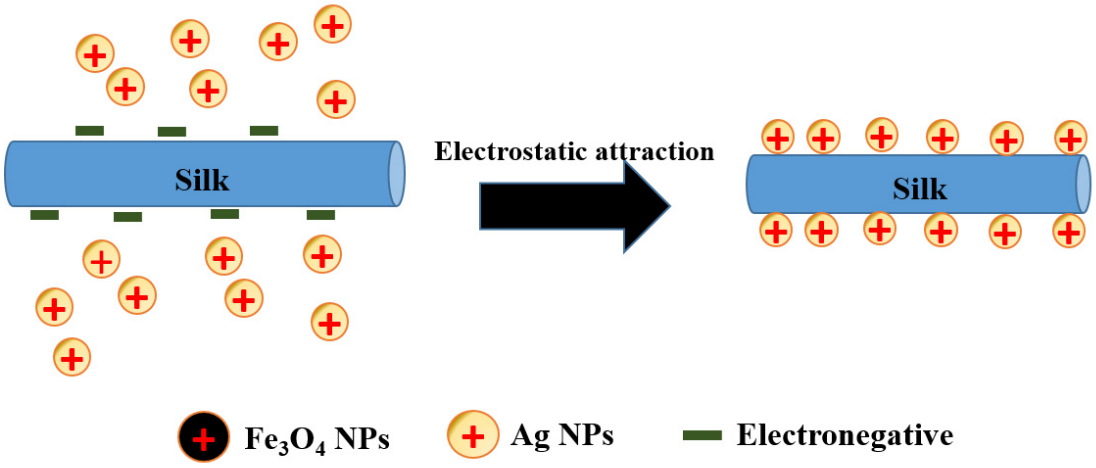

Figure 4.1 Schematic illustration of mechanism of interaction between Ag NPs and silk fibroin.

4.2.2.2 Synthesis of negatively charged GO-Fe_3O_4 NPs [3, 6, 15]

First, 500 mg of GO and five drops of ammonia were added into 200 mL distilled water to form a graphene oxide aqueous dispersion by ultrasonication for 2 h. Meanwhile, 500 mg of octadecylamine (ODA) was dissolved in 100 mL ethanol, and then the solution was added into the graphene oxide aqueous dispersion. Then the reactive system was refluxed at 90 °C with mechanical stirring for 20 h so that GO can be modified by ODA. Second, the temperature of the reaction was turned to 80 °C and the reactive system was purged with N_2. 540.6 mg $FeCl_3 \cdot 6H_2O$ and 198.8 mg $FeCl_2 \cdot 4H_2O$ were added into the reactive system. After reacting for 30 min, 30 mL $NH_3 \cdot H_2O$ (25 wt %) was added into the mixture rapidly. The system was then stirred at 80 °C for 2 h under N_2. Owing to the electrostatic attraction of negative charges on GO and positive charges on the surface of Fe_3O_4 particles, Fe_3O_4 particles grew on the GO surface. Third, with permanent magnets, the product was then washed with excess hot ethanol and water several times to delete excess ODA and free GO in the solution. Finally, citric acid was added to the reaction mixture until to pH=6.3. The as-prepared GO-Fe_3O_4NPs were separated, purified, and redissolved in 200 mL of water. The mechanism of interaction between GO nanosheets and Fe_3O_4 NPs was illustrated in **Figure 4.2**.

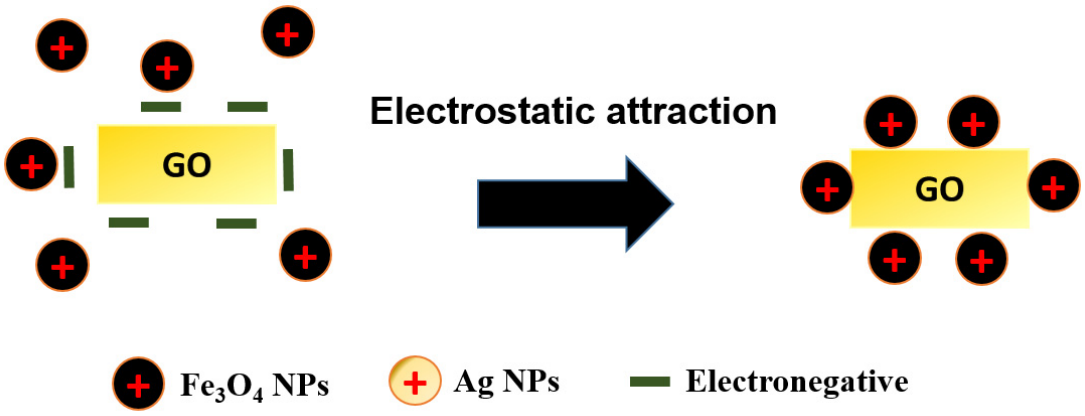

Figure 4.2 Schematic illustration of mechanism of interaction between GO nanosheets and Fe_3O_4 NPs.

4.2.2.3 Preparation of GO-Fe_3O_4NPs/AgNPs dual-coated silk fibers by electrostatic assembly

Silk fibers (0.5 g) were added into 100 mL of AgNP solution (pH=8.4) and kept at 95 °C with constant magnetic stirring for 30 min. The prepared AgNPs coated silk fibers were rinsed in deionized water for several times and air-dried. Next, 0.5 g of AgNPs coated silk fibers were added to 50 mL of GO-Fe_3O_4 colloid solution (pH=6.3) and kept at 35 °C for 10 min. The resulting dual-coated sample was repetitively washed with water and ethanol, and dried under vacuum for 5 h at 50 °C. The mechanism of interaction between GO-Fe_3O_4 and Ag NPs@SFs was illustrated in **Figure 4.3**.

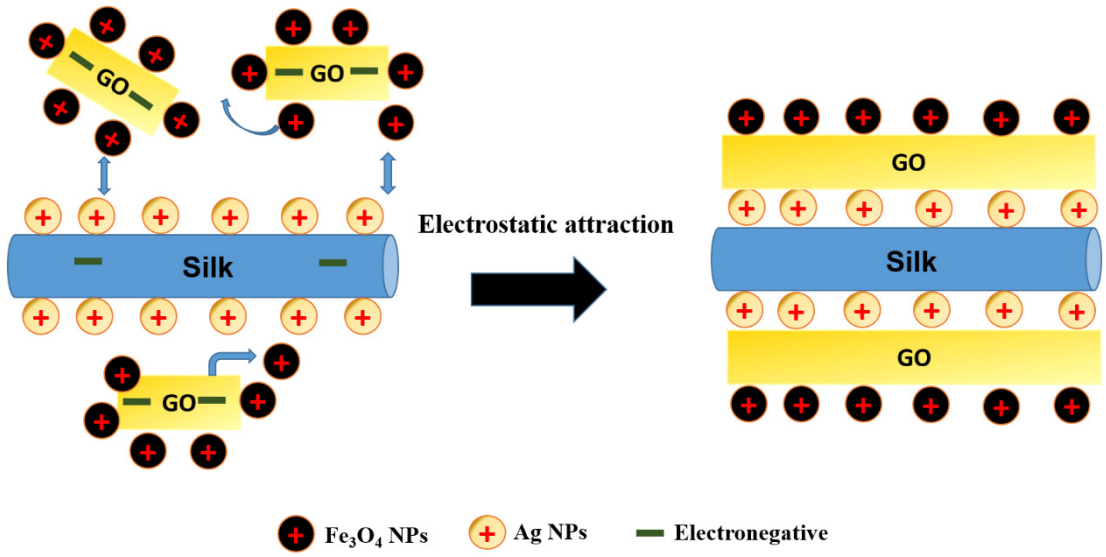

Figure 4.3 Schematic illustration of mechanism of interaction between GO-Fe_3O_4 and Ag NPs@SFs.

4.2.3 Measurements

The morphology and size of AgNPs, GO-Fe_3O_4NPs hybrid nanosheets, and the composite SFs were observed using a field-emission scanning electron microscope (FESEM) (S4800; Hitachi, Japan). The morphology of Fe_3O_4NPs and GO-Fe_3O_4NPs hybrid nanosheets were investigated using a JEOL-2100F transmission electron microscope (TEM) (JEOL, Japan) operating at an accelerating voltage of 120 kV. The chemical composition and surface chemistry of silk fibers and the GO-Fe_3O_4NPs hybrid nanosheets encapsulated AgNP-coated silk fibers were characterized by X-ray photoelectron spectroscopy (XPS) using an X-ray diffractometer (Krotos, Japan, AXIS Ultra DLD) in the region of 0 ~1150 eV.

4.3 Results and discussion

4.3.1 Synthesis of GO-Fe3O4 NPs/AgNPs -coated silk fibers.

The typical synthesis of GO-Fe_3O_4NPs/AgNP-coated silk fibers through self-assembly technology was illustrated in **Figure 4.4**. According to our previous work[6], because of the cationic characteristic of HBPAA and their enhanced intermolecular interactions towards silk fibers and GO due to its three-dimensional structure, dense amino end groups, and low viscosity. HBPAA here serves as a strong guiding agent and glue because of their comparative advantages including cationic and amphipathic characteristics, three-dimensional structure, and dense amino end groups that can capture and fix negatively charged hydroxyl/carboxyl-contained GOs nanosheets compared to linear cationic electrolytes. Meanwhile, based on another our previous work[10], silk fibers were hierarchically coated with HBPAA-capped AgNPs (HBPAA/AgNPs) and GOs by successively impregnating the fibers in the solutions of HBPAA/AgNPs and GOs. In such structure, HBPAA served as a “double-sided tape” not only gluing AgNPs to the fiber surfaces but also adhere GOs to the surfaces of HBPAA/AgNPs. Therefore, the HBPAA-mediated self-assembly showed much greater

loading efficiency than that of cationic linear macromolecules. This advantage makes highly efficient and complete attachment of GOs possible.

Because of Fe_3O_4 nanoparticles with good biocompatibility and low toxicity, and these nanoparticles could be easily recycled without a decrease in their antibacterial activities due to the synergistic effects between the AgNPs and Fe_3O_4NPs with large amounts of active sites. And in order to protect AgNPs coatings from detachment, we designed the graphene oxide (GO)-encapsulated AgNP-coated silk fibers with GO serving as the protective films through HBPAA-directed self-assembly. The employment of ODA plays an important role to effectively prevent the aggregation of Fe_3O_4NPs when Fe_3O_4NPs grow on the surface of GO-ODA in the assembly process.

The potential mechanism is presented in Scheme in **Figure 4.4** shown, hierarchical structured GO-Fe_3O_4NPs/AgNPs bimetallic composite coated silk fibers via a special electrostatic self-assembly technology using positively charged AgNPs and negatively charged GO-Fe_3O_4NPs as the building blocks. Specifically, GO-Fe_3O_4NPs/AgNPs bimetallic composite coated silk fibers were facilely obtained by sequential impregnation with solutions of hyperbranched polyamide (HBPAA)-capped AgNPs and citric acid-capped GO-Fe_3O_4NPs hybrid nanosheets.

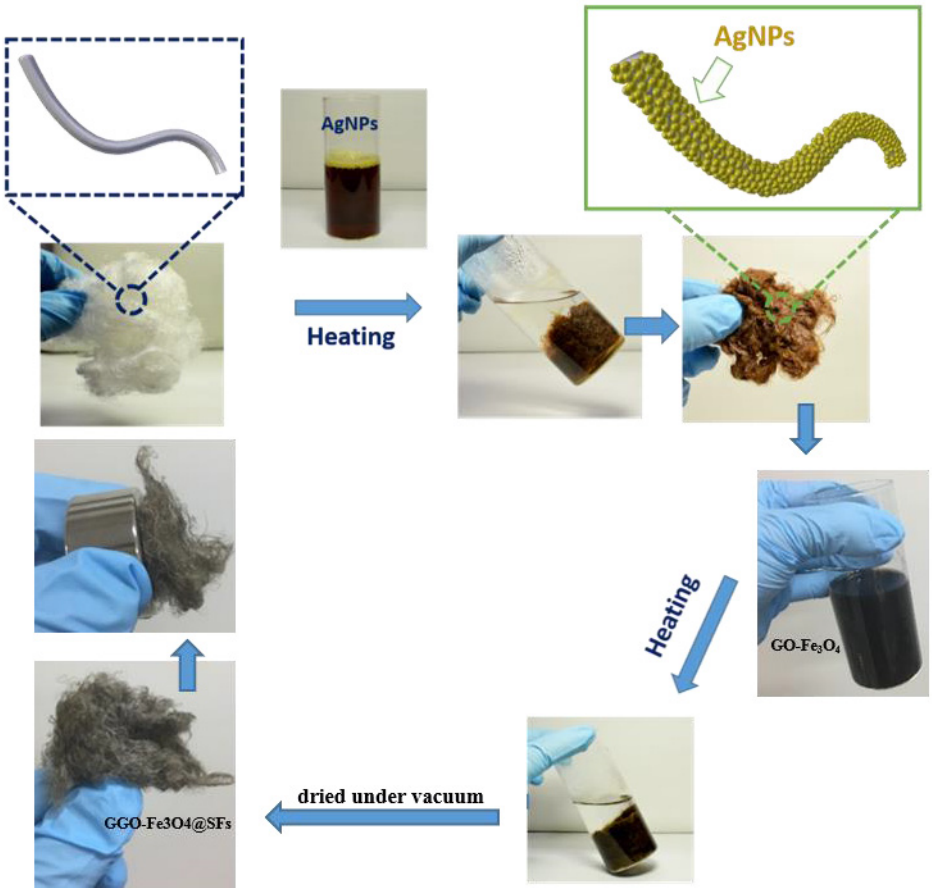

Figure 4.4 Schematic representation of the colloidal self-assembly procedure of GO-Fe_3O_4 NPs/AgNP-coated silk fibers.

4.3.2 TEM analysis

InFigure 4.5a, a micrograph representing a few as-prepared GO-Fe_3O_4NPs hybrid nanosheets, is provided. The graphene sheets with linear dimensions in this image appear to be between 100–300 nm, they are flat and with almost negligible creasing and the graphene layers itself appears to have nanometer size folds especially around the edges. From the red area enlarged view of GO-Fe_3O_4NPs hybrid nanosheets, an HRTEM image of the graphene surrounded by Fe_3O_4 nanoparticles is provided inFigure 4.5b. The Fe_3O_4NPs have a size around 8 nm and they are relatively evenly distributed on the surface of the graphene sheets rather than agglomerated together around certain areas of the graphene sheets due to ODA effectively prevent the aggregation of Fe_3O_4NPs[3]. And representative HRTEM image (**Figure 4.5**b) showing a lattice-fringe spacing of 0.341 nm corresponding to the (111) crystal plane of the sheets. The inset shows the electron diffraction pattern of as-made GOs showing excellent crystallization of the GOs. Meanwhile, slightly distorted, hexagonal-shaped Fe_3O_4NPs with its embedded facets in the GO matrix. The measured lattice-fringes pacing of 0.297 nm and 0.253 nm in these ribbons corresponds to the (220) and (311) crystal plane of the sheets, respectively (see **Figure 4.5**b). All of these results are consistent with those reported in the references [6, 15, 21, 22]. As Fig.4. 2 shown, Fe_3O_4NPs relatively evenly distributed on the surface of the graphene sheets, indicating GO-Fe_3O_4NPs nanosheets were successfully prepared by assembly technology.

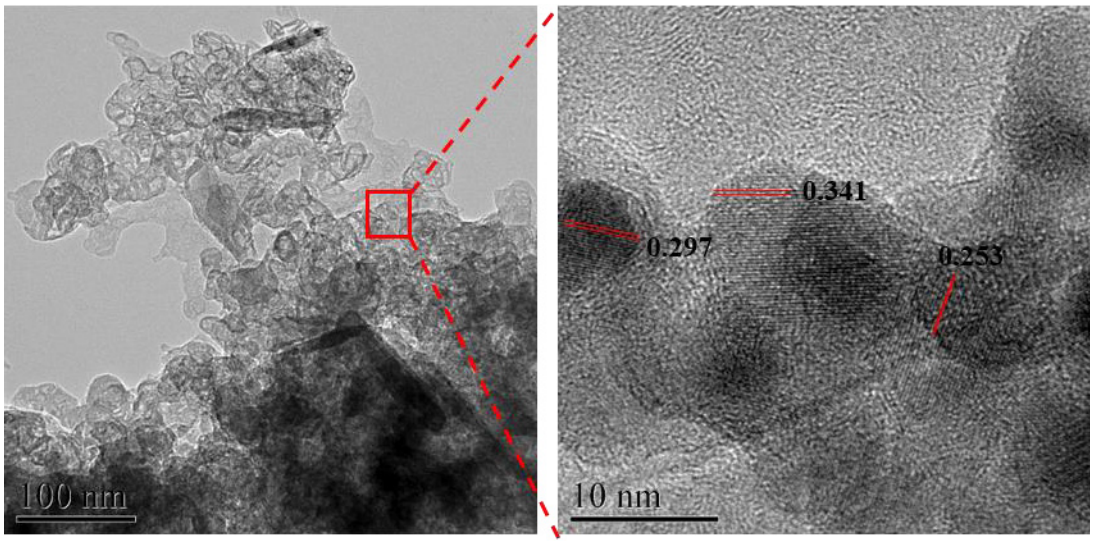

Figure 4.5 Morphological studies of nanocomposites, (a) TEM and high-resolution TEM of as-prepared GO-Fe_3O_4NPs hybrid nanosheets.

4.3.3 FESEM analysis

Comparing to the smooth surface of pristine SF (**Figure 4.6 a**), the surface of AgNPs@SFs was coated uniformly by densely-wrapped spherical NPs with diameters in the range of 1 - 30 nm, as displayed in Fig. 3b and c. The surface texture of silk can be clearly observed from the red area NO.1 enlarged view of AgNPs@SFs, and HBPAA-capped AgNPs densely scattering on the surface of silk fibers, which would make silk and functionalized graphene sheets integrated together tightly in the next process, just as countless solder joints. The whole morphology of the GOs nanosheets with numerous small wrinkles was observed from **Figure 4.6 d - f**. **Figure 4.6d** shows a clean GO sheet having a smooth finish and plenty of wrinkles owing to the thin structure of the sheet. From the red area NO.2 enlarged view of GO-Fe_3O_4NPs nanosheets (**Figure 4.6 e**) in the **Figure 4.6** f, it is clear to observe that densely spherical NPs scattered on the surface of GO nanosheets.

As shown in **Figure 4.6 g – i**, the morphologies and distribution state of AgNPs and Fe_3O_4NPs that are assembled on the surface of GOs and silk fibers was observed by FESEM. Fig. 4.3g and h indicated that GO-Fe_3O_4NPs hybrid nanosheets closely spread on the surface of silk fibers without any self-folding, though excessive stacking was observed in a small part of a silk surface with the increased density of GOs coatings. GO-Fe_3O_4NPs were observed coated the outermost layer of the fiber and Fe_3O_4NPs are uniformly distributed on the graphene oxide. From the red area NO.3 enlarged view of GO-Fe_3O_4NPs/AgNPs@SFs (**Figure 4.6** g), GOs with numerous small wrinkles that were different from the surface texture of silk and a fraction of large buckling deformation were clearly visible, mainly caused by the crimp or warping of GO nanosheets [23]. Except for a small part of large warps, GO-Fe_3O_4NPs nanosheets seem to be closely attached and monodispersed onto silk surface since the surface texture of silk can be clearly seen through these GO films from the red area NO.4 enlarged view of GO-Fe_3O_4NPs/AgNPs@SFs (**Figure 4.6** i), which proved their hierarchical structure.

An obvious hierarchical structure was observed, indicating GO-Fe_3O_4NPs nanosheets were successfully assembled onto the surface of AgNPs@SFs via electrostatic attractions between the positively charged HBPAA-capped AgNPs and negatively charged GO-Fe_3O_4NPs nanosheets.

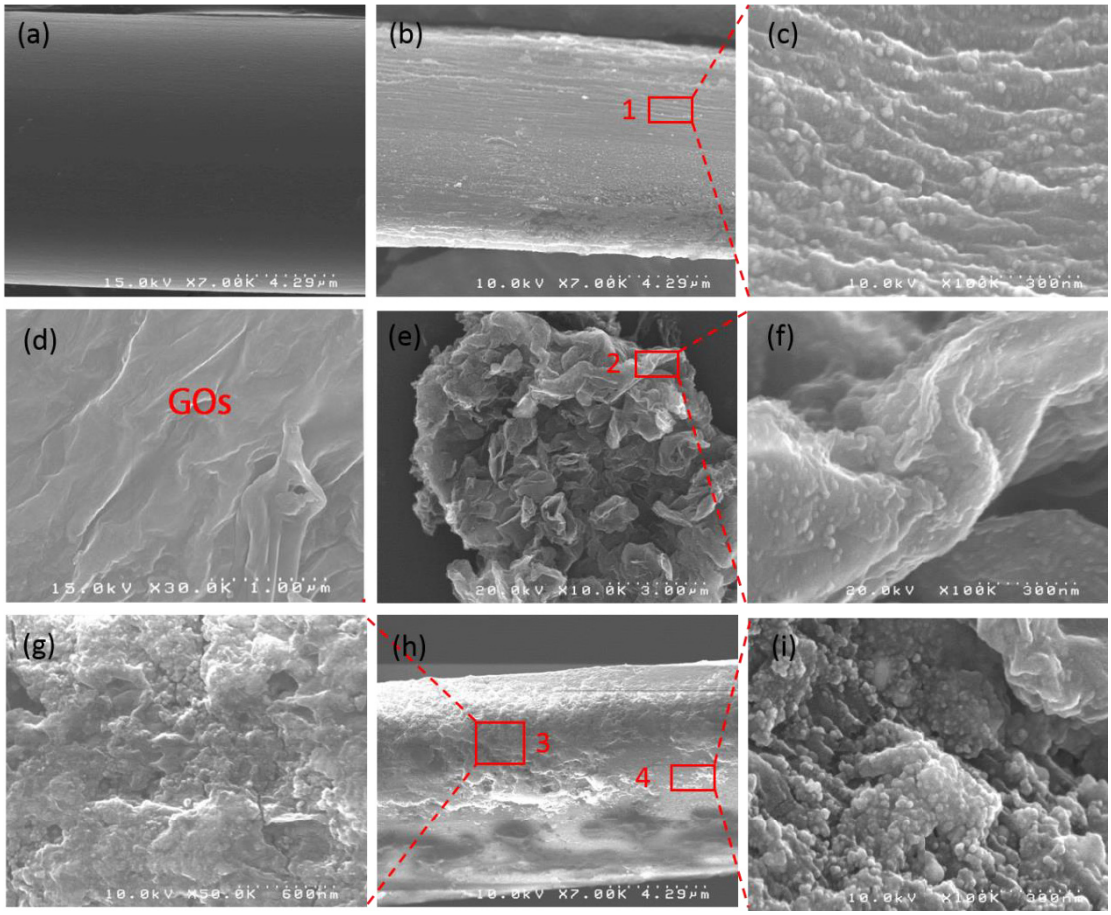

Figure 4.6 FESEM photographs of (a ×7,000) pristine SF, (b ×7,000, c ×50,000) AgNPs@SFs, (d ×30,000) Graphene oxides, (e ×10,000, f ×100,000) GO-Fe_3O_4NPs nanosheets and (g ×50,000, h ×7,000 and i ×100,000) GO-Fe_3O_4NPs/AgNPs@SFs.

4.3.4 XPS analysis

In order to determine the chemical composition and surface chemistry of GO-Fe_3O_4NPs/AgNPs@SFs composite, X-ray photoelectron spectroscopy (XPS) measurements were carried out in the region of 0 ~1150 eV (**Figure 4.7** a). All wide-scan XPS spectra showed photoelectron lines at a binding energy of about 284.5, 399, and 532 eV, attributed to C1s, N1s, and O1s, respectively. They were mainly derived from silk, while it also obviously changed in the chemical composite fibers due to the participation of HBPAA-capped AgNPs and GO-Fe_3O_4NPs. After self-assembly of HBPAA/AgNPs to the silk surfaces and after GO-Fe_3O_4NPs nanosheets-encapsulated, in comparison with pristine silk, the relative intensity of the O1s and N1s bond obviously increased, indicating the successful attachment of amide-rich HBPAA and GO nanosheets. In contrast, the relative intensity of C1s bond slightly decreased, due to Fe_3O_4NPs distributing on the graphene oxide and GO-Fe_3O_4NPs encapsulating the outermost layer of the fiber, which shielded the detection of carbon elements of the GO-Fe_3O_4NPs/AgNPs@SFs composite.

According to the analysis of wide-scan XPS spectrum, the sharp peaks at binding energies 56 eV is related to Fe3p electronic states, and have been appeared as an indication that the samples contain Fe elements. In **Figure 4.7 b**, two distinct peaks of a Fe2p level with binding energies at 710.4 and 723.8 eV were assigned to $Fe2p_{3/2}$ and $Fe2p_{1/2}$ spin-orbit peaks of Fe_3O_4, respectively, which indicates the formation of magnetite nanocomposite (i.e. the Fe_3O_4NPs onto GOs) [15, 24]. In the Ag3d XPS spectra shown in **Figure 4.7** c, the Ag $3d_{3/2}$ and $Ag3d_{5/2}$ peaks of GO-Fe_3O_4NPs nanosheets-encapsulated HBPAA/AgNP-coated silk were both around 374.1 and 368.1 eV, indicating the metallic state of HBPAA/AgNPs [25].

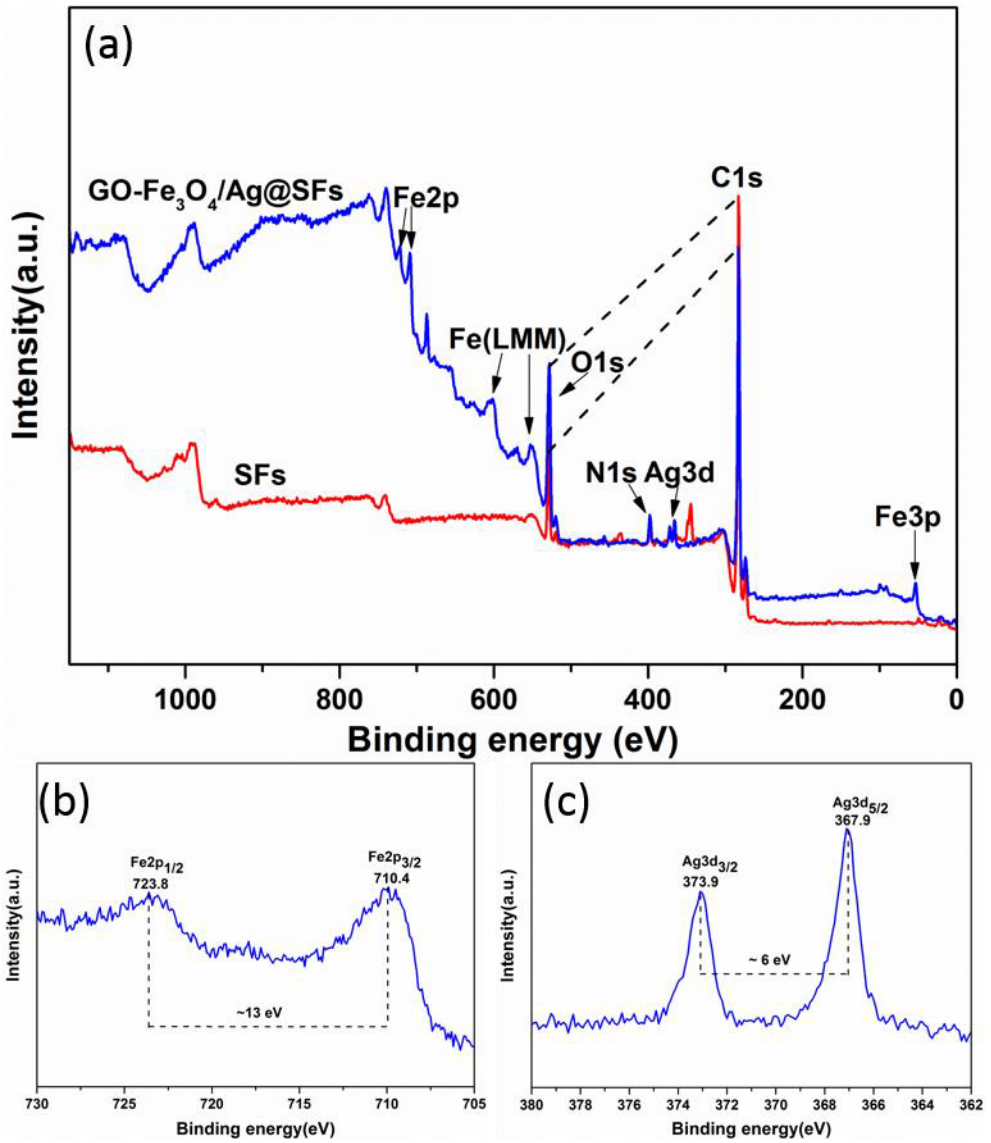

Figure 4.7 (a) Wide-scan XPS spectra of silk fibers (SFs, red) and GO-Fe_3O_4NPs/AgNPs@SFs (blue) nanocomposites silk fibers, (b) Fe2p and (c) Ag3d spectra of the GO-Fe_3O_4NPs/AgNPs@SFs.

4.4. Conclusions

In the present work, special hierarchical structured GO-Fe_3O_4NPs/AgNPs bimetallic coated silk fibers have been prepared via a simple electrostatic self-assembly technology. Silk fibers were sequentially immersed in solutions of positively charged AgNPs and negatively charged GO-Fe_3O_4NPs as the building blocks. As-prepared hierarchical structured silk fibers were characterized by XRD, SEM and FESEM. XRD and SEM characterizations demonstrated that silk fibers were hierarchically and uniformly coated by high dense AgNPs and Fe_3O_4NPs. Results from XRD showed that GO- Fe_3O_4NPs and AgNPs were anchored onto the surface of silk fibers. FESEM displayed that the high dense GO-Fe_3O_4NPs and AgNPs were hierarchically coated on the fiber surface. The as-prepared bimetallic coated silk fibers exhibited excellent magnetic property, which can be attributed to the high dense Fe_3O_4NPs assembled on the surface of silk fibers, and durable antibacterial property, which can be attributed to the high dense AgNPs assembled on the surface of silk fibers and protection from a robust, hard, and closely-fitted protective films of GO-Fe_3O_4NPs.

References

[1] Dallas P, Tucek J, Jancik D, Kolar M, Panacek A, Zboril R. Magnetically Controllable Silver Nanocomposite with Multifunctional Phosphotriazine Matrix and High Antimicrobial Activity. Advanced Functional Materials. 2010;20:2347-54.

[2] Zhan Y, Wan X, Long Z, Fan Y, He Y. Two step hydrothermal synthesis of flowerbud-like magnetite/graphene oxide hybrid with high-performance microwave absorption. Russian Journal of Applied Chemistry. 2016;89:297-303.

[3] Zha J-W, Huang W, Wang S-J, Zhang D-L, Li RKY, Dang Z-M. Difunctional Graphene-Fe3O4Hybrid Nanosheet/Polydimethylsiloxane Nanocomposites with High Positive Piezoresistive and Superparamagnetism Properties as Flexible Touch Sensors. Advanced Materials Interfaces. 2016;3:1500418.

[4] Alvand M, Shemirani F. Fabrication of Fe3O4@graphene oxide core-shell nanospheres for ferrofluid-based dispersive solid phase extraction as exemplified for Cd(II) as a model analyte. Microchimica Acta. 2016;183:1749-57.

[5] Liu X, Yin G, Yi Z, Duan T. Silk Fiber as the Support and Reductant for the Facile Synthesis of Ag–Fe3O4 Nanocomposites and Its Antibacterial Properties. Materials. 2016;9:501.

[6] Xu S, Song J, Morikawa H, Chen Y, Lin H. Fabrication of hierarchical structured Fe3O4 and Ag nanoparticles dual-coated silk fibers through electrostatic self-assembly. Materials Letters. 2016;164:274-7.

[7] Mehdinia A, Rouhani S, Mozaffari S. Microwave-assisted synthesis of reduced graphene oxide decorated with magnetite and gold nanoparticles, and its application to solid-phase extraction of organochlorine pesticides. Microchimica Acta. 2016;183:1177-85.

[8] Tao H, Kaplan DL, Omenetto FG. Silk Materials – A Road to Sustainable High Technology. Advanced materials. 2012;24:2824-37.

[9] Fei X, Jia M, Du X, Yang Y, Zhang R, Shao Z, et al. Green synthesis of silk fibroin-silver nanoparticle composites with effective antibacterial and biofilm-disrupting properties. Biomacromolecules. 2013;14:4483-8.

[10] Xu S, Song J, Zhu C, Morikawa H. Graphene oxide-encapsulated Ag nanoparticle-coated silk fibers with hierarchical coaxial cable structure fabricated by the molecule-directed self-assembly. Materials Letters. 2016.

[11] Chen D, Ji G, Ma Y, Lee JY, Lu J. Graphene-encapsulated hollow Fe(3)O(4) nanoparticle aggregates as a high-performance anode material for lithium ion batteries. ACS applied materials & interfaces. 2011;3:3078-83.

[12] Ai L, Zhang C, Chen Z. Removal of methylene blue from aqueous solution by a solvothermal-synthesized graphene/magnetite composite. Journal of hazardous materials. 2011;192:1515-24.

[13] Li X, Huang X, Liu D, Wang X, Song S, Zhou L, et al. Synthesis of 3D Hierarchical Fe3O4/Graphene Composites with High Lithium Storage Capacity and for Controlled Drug Delivery. The Journal of Physical Chemistry C. 2011;115:21567-73.

[14] Li J, Zhang S, Chen C, Zhao G, Yang X, Li J, et al. Removal of Cu(II) and fulvic acid by graphene oxide nanosheets decorated with Fe3O4 nanoparticles. ACS applied materials & interfaces. 2012;4:4991-5000.

[15] Eskusson J, Rauwel P, Nerut J, Jänes A. A Hybrid Capacitor Based on Fe3O4-Graphene Nanocomposite/Few-Layer Graphene in Different Aqueous Electrolytes. Journal of The Electrochemical Society. 2016;163:A2768-A75.

[16] Xu S, Chen S, Zhang F, Jiao C, Song J, Chen Y, et al. Preparation and controlled coating of hydroxyl-modified silver nanoparticles on silk fibers through intermolecular interaction-induced self-assembly. Materials & Design. 2016;95:107-18.

[17] Tung VC, Allen MJ, Yang Y, Kaner RB. High-throughput solution processing of large-scale graphene. Nature nanotechnology. 2009;4:25-9.

[18] Chen J, Yao B, Li C, Shi G. An improved Hummers method for eco-friendly synthesis of graphene oxide. Carbon. 2013;64:225-9.

[19] Shahriary L, Athawale AA. Graphene oxide synthesized by using modified hummers approach. IJREEE. 2014;2:58-63.

[20] Jiaqing X, Chenlu J, Sijun X, Jin T, Desuo Z, Hong L, et al. Strength-controllable graphene oxide amphiprotic aerogels as highly efficient carrier for anionic and cationic azo molecules. Japanese Journal of Applied Physics. 2015;54:06FF7.

[21] Pasricha R, Gupta S, Srivastava AK. A facile and novel synthesis of Ag-graphene-based nanocomposites. Small. 2009;5:2253-9.

[22] Jiang P, Yang X, Xin Y, Qi Y, Ma X, Li Q, et al. Facile synthesis of water-soluble and superparamagnetic Fe3O4 dots through a polyol-hydrolysis route. Journal of Materials Science. 2012;48:2365-9.

[23] Suresh I, Chidambaram K, Vinod V, Rajender N, Venkateswara RM, Miroslav Č. Synthesis, characterization and optical properties of graphene oxide–polystyrene nanocomposites. Polymers for Advanced Technologies. 2015;26:214-22.

[24] Lu J, Jiao X, Chen D, Li W. Solvothermal synthesis and characterization of Fe3O4 and γ-Fe2O3 nanoplates. The Journal of Physical Chemistry C. 2009;113:4012-7.

[25] Zhao S, Cheng Z, Kang L, Zhang Y, Zhao X. A novel preparation of porous spong-shaped Ag/ZnO heterostructures and their potent photocatalytic degradation efficiency. Materials Letters. 2016;182:305-8.

Chapter 5: Conclusion

Chapter 5 Conclusion

Silk is a kind of high strength natural filament fiber material with good mechanical properties; silk protein is not toxic and harmless and has good biocompatibility and degradation. However, because of the single structure, it limits the application of silk materials. Thus improving silk performance, preparation of silk/nano ions composite materials, in the development of new features of silk is of great significance. Graphene and graphene-based materials have recently gained extensive interests for their good application potential in composite nanomaterials because of their unique physicochemical properties. Due to the poor affinity of graphene to natural fibers, naked functional nanoparticle coatings on natural fibers usually suffer from a function decrease under external physical and chemical stimuli, thereby leading to a poor function durability. In the research, understanding the compatibility between nature silk and functional nanomaterials (including graphene-based materials and functional nanoparticles) is essential to advance the use of silk in functional applications. Compared with the traditional regenerated silk blend nanocomposites, the study of silk material the preparation does not change the internal structure of silk fibroin, fully retained the excellent characters of natural silk.

Silk is tough, but it becomes soft when exposed to water. Here a strong affinity of amine-functionalized Graphene oxide (AFGO) was designed, by coating the silk fibers with AFGO by self-assembly technique onto the silk fibers to prepare of AFGO @ silk composites using self-assembly technique. And then, a special layer-by-layer (LbL) assembly technology was developed to prepare a tightly-adhered GOs coating. Particular, a GOs coating was prepared by cycle impregnation of two separate solutions of hyperbranched poly(amide-amine) (HBPAA) and GOs. HBPAA here serves as a strong guiding agent and glue because of their comparative advantages including cationic and amphipathic characteristics, three-dimensional structure, and dense amino

end groups that can capture and fix negatively charged hydroxyl/carboxyl-contained GOs nanosheets compared to linear cationic electrolytes. The developed LbL self-assembly technology may provide a controllable approach to coat GOs on the surface of biological fibers and graphene- based functional materials. At the same time, the prepared graphene and silk composite fiber can serve as the carrier of functional composite fibers, which has increased the chances of more choices to develop multi-functional composite fibers.

In Chapter 2, graphene oxide (GO)-coated silk fibers were fabricated through HBPAA-induced LbL self-assembly technology. The closely adhered GOs coatings were achieved by circular incubation with solutions of HBPAA and GOs, with HBPAA serving as the "molecular glue" that could bind single or multi-layered GOs to the surface of silk fibers. We detailedly demonstrated LbL assembly process. The surface chemical and physical properties of designed GOs /HBPAA-coated silk fibers were also characterized. In the experiments, GOs nanosheets were synthesized by a modified Hummers method and were characterized by atomic force microscopy (AFM), transmission electron microscopy (TEM), X-ray diffraction (XRD), and X-ray photoelectron spectroscopy (XPS). Our developed technology was able to tightly bind GOs to the silk surface and control their loading capacity. Owing to the positive charges and abundant amino end groups of HBPAA, GOs were found to be completely adsorbed onto silk surface. Therefore, their assembly would be green and controllable. The Fourier transform infrared (FT-IR) spectroscopy, XPS, XRD, thermos-gravimetric characterizations confirmed the attachment of HBPAA and GOs. Field emission scanning electron microscopy (FESEM) indicated that GOs closely spread on the surface of silk fibers without any self-folding though excessive stacking was observed in a small part of a silk surface with the increased density of GOs coatings.

In chapter 3, for protecting Ag NP coatings from detachment, we designed the graphene oxide (GO)-encapsulated Ag nanoparticle (Ag NP)-coated silk fibers with GO serving as the protective films through HBPAA-directed self-assembly. By introducing

two dimensional GO nanosheets, a robust, hard, and closely-fitted protective films can be achieved on the fiber surfaces through self-stacked GOs were also found. To design a well-defined hierarchical structure, silk fibers were hierarchically coated with HBPAA-capped Ag NPs (HBPAA/Ag NPs) and GOs by successively impregnating the fibers in the solutions of HBPAA/Ag NPs and GOs. In such structure, HBPAA served as a "double-sided tape" not only gluing Ag NPs to the fiber surfaces but also adhere GOs to the surfaces of HBPAA/Ag NPs. Our FESEM analysis suggested that the ternary silk composites possessed dense mono-dispersed HBPAA/Ag NPs coatings closely encapsulated by GOs. XPS and XRD characterizations showed that large amounts of GOs were successfully coated to metallic Ag NP surfaces. The developed coaxial cable-structured coatings could isolate Ag nanocoatings from external stimuli, opening a potential route to improve the function persistence and biosafety of Ag NP-coated bio textiles.

In chapter 4, design and fabrication of well-organized hierarchical structured graphene oxide (GO)-Fe_3O_4 hybrid nanosheets and Ag nanoparticles (Ag NPs) bimetallic coated silk fibers via a facile and simple assembly technology remain a significant challenge. Here we prepared novel hierarchical structured GO-Fe_3O_4 NPs /Ag NPs bimetallic coated silk fibers via a special electrostatic self-assembly technology using positively charged Ag NPs and negatively charged GO-Fe_3O_4 NPs as the building blocks. Specifically, GO-Fe_3O_4 NPs/Ag NPs bimetallic coated silk fibers were facilely obtained by sequential impregnation with solutions of HBPAA-capped Ag NPs and citric acid-capped GO-Fe_3O_4 NPs. In the present work, special hierarchical structured GO-Fe_3O_4 NPs/Ag NPs bimetallic coated silk fibers have been prepared via a simple electrostatic self-assembly technology. Silk fibers were sequentially immersed in solutions of positively charged Ag NPs and negatively charged GO-Fe_3O_4 NPs as the building blocks. As-prepared hierarchical structured silk fibers were characterized by XRD, SEM, and FESEM. XRD and SEM characterizations demonstrated that silk fibers were hierarchically and uniformly coated by high dense Ag NPs and Fe_3O_4 NPs. Results

from XRD showed that GO- Fe_3O_4 NPs and Ag NPs were anchored onto the surface of silk fibers. FESEM displayed that the high dense GO-Fe_3O_4 NPs and Ag NPs were hierarchically coated on the fiber surface. The as-prepared bimetallic coated silk fibers exhibited excellent magnetic property, which can be attributed to the high dense Fe_3O_4 NPs assembled on the surface of silk fibers, and durable antibacterial property, which can be attributed to the high dense Ag NPs assembled on the surface of silk fibers and protection from a robust, hard, and closely-fitted protective films of GO-Fe_3O_4 NPs.

In this study, we prepared three kinds of silk nanocomposites, such as GO-coated silk fibers, GO-encapsulated Ag NP-coated silk fibers, and GO-Fe_3O_4 NPs/Ag NPs bimetallic coated silk fibers through LbL self-assembly technology of graphene oxide, silver nanoparticles and Fe_3O_4 NPs coating on natural silk surface. The surface coating materials can be controlled and assembled quantitatively by the number of cross-linking / adsorption, HBPAA as a molecular glue in the course of the study, which is simple and easy to implement. Compared with the traditional regenerated silk blending nanocomposites, it is not necessary to dissolve and regenerate of silk, which eliminates the cumbersome process of experiment. At the same time, because the Nano ions are not embedded in silk fibroin, the as-prepared silk composite materials are coated with Nano ions outside the silk fiber. Therefore, the preparation of silk composite materials does not change the internal structure of silk fibroin, which fully retains the excellent characters and shape of natural silk. The experiment was the first, and no other reports have been reported before.

Because the polyamine group has the opposite charge of the Nano ion, the preparation of nanocomposite materials is strong and not easy to fall off, and it is easier to give full play to the performance of the surface nanomaterials. Moreover, because the silk itself has good mechanical performance, stable physical and chemical properties and good biocompatibility, so the as-prepared silk nanomaterial fibers can be made of silk by the modern textile technology, in turn, which makes the original fiber material weaved all kinds of fabric with the corresponding fabric structure. This material also

can be used as the raw material for medical gauze or protective clothing, because of the excellent antibacterial properties of nanomaterials such as graphene and Nano silver. Therefore, the silk nanomaterial fiber with good performance has a vast prospect in various fields. This study has shed a light on the new research of silk nanomaterials, and also provided direction and data support for the new application of silk fiber as the traditional natural fiber.

In addition, due to the haste of time, there are still many parts to be improved, so in the next step, we will continue to supplement and develop the current research: 1. In-depth study of the interaction between the functional materials and bacteria of the silky nanometer and the antimicrobial activity mechanism of the silk nanomaterials. 2. To study the textile technology of the application and development of the functional silk-based materials, providing reference and support for the application in more fields.

Chapter 6: Acknowledge

Acknowledge

It is my pleasure to write this message and express my gratitude to all those who have directly or indirectly contributed to the creation of this thesis.

First and foremost, I would like to express my deepest gratitude to Prof. Hideaki Morikawa, my supervisor, for his great enthusiasm and infinite patience, valuable guidance and large support through my doctoral course in Shinshu University. Special thanks are given to Prof. Shigeru Yamanaka, Prof. Yasushi Tamada, Prof. Hisanao Usami and Prof. Chunhong Zhu for their continuous instruction with the important suggestion, precious advice as well as their enduring patience, fruitful encouragement.

I would like to express my gratitude to the reviewers, Prof. Okino, Prof. Tamada, Prof. Usami, and Prof. Gotoh for their kind supports and their invaluable comments and insights which provided significant support on this work.

I also acknowledge with pleasure to Ms. Nakamura, Ms. Shinotsuka, and Ms. Nishida for assistance with the experiments and also thank Mr. Isaka, Mr. Shimizi, Mr. Koyama, Ms. Machiya, and Ms. Suzuki for patience and help.

I would like to thank my colleagues in Morikawa Laboratory for their generous assistance in every aspect of my life and warm encouragement like family during my study in Japan. Of course, thanks also would be given to my dear friends of Chinese students during learning career in Ueda. Whether living or learning, they often help me. Whether happy or hardship, they always accompany me. I am so lucky as to meet lots of kind friends during learning career in Ueda.

I dedicate my greatest thanks to my beloved family. My parents' encouragement, the love of my wife, and the sweet smile of my son are my greatest motivation. I can not express my deep gratitude to my parents for their patience, understanding, love, and unlimited support over the years.

Chapter 7: List of publications

[1]. **Jiangchao Song**, Sijun Xu, Tao Chen, Shigeru Yamanaka, Hideaki Morikawa. Preparation of graphene oxide-coated silk fibers through HBPAA [a molecular glue]-induced layer-by-layer self-assembly. Journal of the Iranian Chemical Society. https://doi.org/10.1007/s13738-017-1213-y, 2017.

[2]. Sijun Xu, **Jiangchao Song**, Chunhong Zhu, Hideaki Morikawa. Graphene oxide-encapsulated Ag nanoparticle-coated silk fibers with hierarchical coaxial cable structure fabricated by the molecule-directed self-assembly. Materials Letters, 188: 215-219, 2017.

[3]. **Jiangchao Song,** Sijun Xu, Tao Chen, Hideaki Morikawa. Fabrication of hierarchical structured graphene oxide-Fe_3O_4 hybrid nanosheets and Ag nanoparticles bimetallic composite coated silk fibers through self-assembly. Journal of Silk Science and Technology of Japan, 25: 59-68, 2017.